1000-0569/2018/034(06)-1612-40 *Acta Petrologica Sinica* 岩石学报

灵山岛早白垩世岩浆活动及其大地构造意义*

敖文昊[1] 冯涛[2] 赵燕[1] 翟明国[1,3] 孙勇[1]

AO WenHao[1], FENG Tao[2], ZHAO Yan[1], ZHAI MingGuo[1,3] and SUN Yong[1]

1. 大陆动力学国家重点实验室,西北大学地质学系,西安 710069
2. 磐金国际资源有限公司,香港 999077
3. 中国科学院计算地球动力学重点实验室,中国科学院大学地球与行星科学学院,北京 100049
1. *State Key Laboratory of Continental Dynamics, Department of Geology, Northwest University, Xi'an* 710069, *China*
2. *Pangea Gold Corporation Limited, Kowloon, Hong Kong* 999077, *China*
3. *Key Laboratory of Computational Geodynamics, College of Earth and Planetary Sciences, University of Chinese Academy of Sciences, Beijing* 100049, *China*

2017-12-19 收稿, 2018-03-07 改回.

Ao WH, Feng T, Zhao Y, Zhai MG and Sun Y. 2018. Early Cretaceous magmatic activities in the Lingshan Island and its geological significance. *Acta Petrologica Sinica*, 34(6): 1612-1640

Abstract The Lingshan Island is located approximately 16km in the south of Jiaodong Peninsula. It is known as the eastern part of the Dabie-Sulu orongenic belt conjuncting the North China Craton (NCC) and the Yangtze Block (YB). In Late Early Cretaceous, magmatic activities strongly occurred in this place, developing numerous rhyolites and volcanic breccias in the upper part of the island that unconformably overlies the clastic sedimentary rocks in the lower part. What's more, mafic dyke swarms (diabase porphyrite) widely intrude into the clastic sedimentary rocks along the NE-SW trend. In this study, petrogeochemical and chronological analyses were conducted on the rhyolite and diabase porphyrite. The results show that the rhyolite samples have high K_2O contents (4.10% ~ 4.42%) and are alkali-rich ($Na_2O + K_2O = 8.83\% \sim 9.06\%$), with low contents of CaO (0.10% ~ 0.46%), TiO_2 (0.08% ~ 0.09%), MgO (0.12% ~ 0.15%) and $Fe_2O_3^T$ (0.79% ~ 0.83%). All the samples are slightly peraluminous and belong to calcic-alkaline rock series. Their chondrite-normalized REE patterns are characterized by slightly enrichment of LREEs ($(La/Yb)_N = 6.42 \sim 8.09$), relatively low REE contents ($\sum REE = 109.0 \times 10^{-6} \sim 128.8 \times 10^{-6}$) and negative Eu anomalies ($\delta Eu = 0.27 \sim 0.28$). The diabase porphyrite samples have low SiO_2 contents (51.17% ~ 51.97%), high alkali contents ($Na_2O + K_2O = 5.01\% \sim 6.07\%$) and $Mg^{\#}$ values (67.6 ~ 69.4), belonging to shoshonitic rock series. Their chondrite-normalized REE patterns show relatively enrichment of LREEs ($(La/Yb)_N = 11.1 \sim 11.6$) and relatively high REE contents ($\sum REE = 160.6 \times 10^{-6} \sim 173.5 \times 10^{-6}$), with slightly positive Eu anomalies ($\delta Eu = 1.12 \sim 1.18$). In the primitive mantle-normalized trace element patterns and chondrite-normalized REE patterns, these diabase porphyrite samples display OIB affinity. All these geochemical features reveal that the rhyolite and diabase porphyrite were generated in an extentional setting with low pressure. Futhermore, LA-ICP-MS zircon U-Pb dating results show that the rhyolite and diabase porphyrite were produced by Early Cretaceous magmatism, with formation age of 118 ± 2Ma and 109 ± 3Ma, respectively. Zircon Lu-Hf isotopic analyses indicate that the rhyolite was derived from an ancient crustal origin with negative $\varepsilon_{Hf}(t)$ values of $-31.0 \sim -24.5$, while the diabase porphyrite was derived from the enriched mantle source with negative $\varepsilon_{Hf}(t)$ values of $-31.2 \sim -28.8$ which mingled by deep depleted mantle components with positive $\varepsilon_{Hf}(t)$ values of $+7.1 \sim +8.1$. All these signatures, together with regional contemporary tectonic events suggest that, affected by the direction-changed of subduction of Izanagi plate and paleo-Pacific plate, tectonic regime in eastern China was transformed during Mesozoic. In Late Early Cretaceous, the eastern NCC was under extensional regime, producing a series of rhyolites and diabase porphyrite dykes, which represent geological response to the Yanshan Movement in Jiaodong Peninsula.

Key words Lingshan Island; Early Cretaceous; Yanshan Movement; Cratonic destruction

摘 要 灵山岛位于胶东半岛以南约16km处,构造上处于扬子和华北克拉通结合部位——苏鲁造山带东端。早白垩世晚

* 本文受国家"973"项目(2012CB416606)和西北大学大陆动力学国家重点实验室科技部专项联合资助.

第一作者简介: 敖文昊,男,1989年生,博士生,地球化学专业,E-mail: awhheye@126.com

期，灵山岛岩浆活动极为强烈，大量发育流纹岩和火山角砾岩，不整合覆盖于底部碎屑沉积岩层之上；同时，区内广泛发育基性岩墙（辉绿玢岩），沿北东-南西向侵入于碎屑沉积岩地层之中。本文选取流纹岩和辉绿玢岩样品进行了岩石地球化学和年代学研究。结果表明，流纹岩具有富钾（K_2O = 4.10% ~ 4.42%）、富碱（$Na_2O + K_2O$ = 8.83% ~ 9.06%）、贫钙（CaO = 0.10% ~ 0.46%）、低钛（TiO_2 = 0.08% ~ 0.09%）、低镁（MgO = 0.12% ~ 0.15%）和铁（$Fe_2O_3^T$ = 0.79% ~ 0.83%）的特征，属于弱过铝质高钾钙碱性岩石系列；岩石稀土总量较低（$\sum REE = 109.0 \times 10^{-6} \sim 128.8 \times 10^{-6}$），轻重稀土元素分异较弱（$(La/Yb)_N$ = 6.42 ~ 8.09），Eu 显著负异常（δEu = 0.27 ~ 0.28）。辉绿玢岩 SiO_2 含量为（51.17% ~ 51.97%），具有富碱（$Na_2O + K_2O$ = 5.01% ~ 6.07%）和高 $Mg^{\#}$ 值（67.6 ~ 69.4）的特征，属于钾玄岩系列；岩石稀土总量较高（$\sum REE = 160.6 \times 10^{-6} \sim 173.5 \times 10^{-6}$），轻重稀土元素分馏较为明显（$(La/Yb)_N$ = 11.1 ~ 11.6），显示弱 Eu 正异常（δEu = 1.12 ~ 1.18），它们在球粒陨石标准化稀土元素图解和原始地幔标准化微量元素图解上与 OIB 类似。上述地球化学特征指示流纹岩和辉绿玢岩可能均形成于伸展减压背景下。LA-ICP-MS 锆石 U-Pb 定年结果表明，流纹岩和辉绿玢岩的形成时代分别为 118 ± 2Ma 和 109 ± 3Ma，属于早白垩世岩浆活动的产物。锆石 Hf 同位素分析结果显示，流纹岩具有负的 $\varepsilon_{Hf}(t)$ 值（-31.0 ~ -24.5），表明其来源于古老地壳物质部分熔融。辉绿玢岩的岩浆锆石具有负的 $\varepsilon_{Hf}(t)$ 值（-31.2 ~ -28.8）和正的 $\varepsilon_{Hf}(t)$ 值（+7.1 ~ +8.1），指示其来源于有深部亏损软流圈地幔物质加入的富集地幔源区。综合本文研究结果和同时期区域构造演化推测，受伊泽奈崎板块和古太平洋板块俯冲方向改变的影响，中生代期间中国东部构造体制发生转变。早白垩世晚期，华北东部处于伸展构造背景，形成了一系列与之对应的超浅成相-喷出相辉绿玢岩岩墙和流纹岩，是燕山运动在胶东地区的地质表现。

关键词 灵山岛；早白垩世；燕山运动；克拉通破坏

中图法分类号 P588.124; P588.141; P597.3

灵山岛位于山东省青岛市黄岛以南约 16km 处，构造上处于扬子板块与华北板块之间的结合部位（图 1）。受古太平洋板块俯冲的影响，中国东部发育一系列燕山期岩浆活动。关于灵山岛，吕洪波等（2011，2012）最早报道了该区早白垩世深海复理石沉积以及滑塌褶皱。后续众多学者对灵山岛进行了进一步的相关研究和报道，主要聚焦于灵山岛滑塌沉积构造和软沉积变形（吕洪波等，2011；董晓朋等，2013，2014；王安东，2013；周瑶琪等，2015a，2017；葛毓柱等，2015；张风霄，2015；Feng *et al.*，2016；Yang and Van Loon，2016；冯增昭等，2017；梁钊和周瑶琪，2017）、构造-应力解析（李杰等，2015；张振凯等，2016）、古地理环境（张振凯等，2017）和古生物化石（李守军等，2017）等方面，并由此引发了灵山岛早白垩世沉积环境的海相和陆相之争（高兴辰，1991；钟建华，2012；吕洪波等，2011，2012，2013；邵珠福等，2014a，b；钟建华等，2016）。吕洪波等（2011，2012）认为灵山岛浊积岩和滑塌沉积岩层是中国东部晚中生代海相沉积的代表，并据此推测扬子板块与华北板块的最终闭合在早白垩世仍未完成，期间存在一系列的残留洋盆。这一观点与前人所认为的扬子板块与华北板块于三叠纪已碰撞闭合造山的观点（Ames *et al.*，1996；李曙光等，1996，1997；Hacker *et al.*，1998；刘福来等，2003）有明显差异。张海春等（2013）依据灵山岛早白垩世浊积岩与同时期邻近地层均无法对比的地质现象，提出建立一套新的岩石地层单位——灵山岛组（K_1*lsd*），并将其时代限定为早白垩世早中期，但是不排除其下部有晚侏罗世沉积的可能。钟建华（钟建华，2012；钟建华等，2016）在灵山岛软沉积地层中发现了镜煤细层和炭化的植物碎屑以及风暴岩和风暴沉积，提出这套地层形成于陆相环境，其变形构造与华北板块和扬子板块的碰撞没有任何关系。李守军等（2017）在灵山岛下白垩统泥岩中发现了鱼类和叶肢介化石，确认这套地层属于陆相沉积。邵珠福等（2014a，b）结合沉积构造和岩性、岩相组合研究，认为灵山岛的沉积岩是在内陆三角洲环境形成的，而不是深水环境，更不是海底斜坡，与华北板块和扬子板块的碰撞无关。由此可见，关于灵山岛早白垩世地层的沉积环境和成因等目前还存在很大争议，这一问题间接影响了对灵山岛中生代大地构造背景的认识。

灵山岛地层的形成时代目前已有较为确切年代学证据，Wang *et al.*（2014）和周瑶琪等（2015b）分别获得岛上流纹岩的形成时代为 123.9 ± 1.6Ma 和 119.2 ± 2.2Ma。Wang *et al.*（2014）通过沉积地层碎屑锆石的研究，将地层最大沉积时代划为 138 ~ 121Ma。然而，前人的研究很少有关于灵山岛火山岩地球化学以及基性岩墙年代学和地球化学研究的报道，这些岩浆活动对限定灵山岛中生代地层沉积时代、壳幔相互作用及区域大地构造背景等具有重要指示意义。因此，本文以此为切入点，在野外地质调研的基础上，选取灵山岛典型白色流纹岩和基性侵入岩墙样品，进行岩石地球化学、LA-ICP-MS 锆石 U-Pb 年代学和锆石 Hf 同位素分析，以期为探讨灵山岛早白垩世晚期岩浆活动的地球深部动力学机制及其大地构造意义提供证据。

1 区域地质背景

灵山岛处于扬子地块与华北地块的重要结合部位——苏鲁造山带东端（图 1a，b）。该地区西部紧邻郯庐断裂带，北部和南部受五莲-烟台（牟平）和千里岩断裂控制，发育多条呈 NNE 向平行分布的主断层，基本构造格架为盆岭相间出现，从北到南依次为胶北隆起、胶莱盆地和胶南隆起（图 1a）。胶莱盆地是白垩纪的断陷盆地，其北部的胶北隆起属

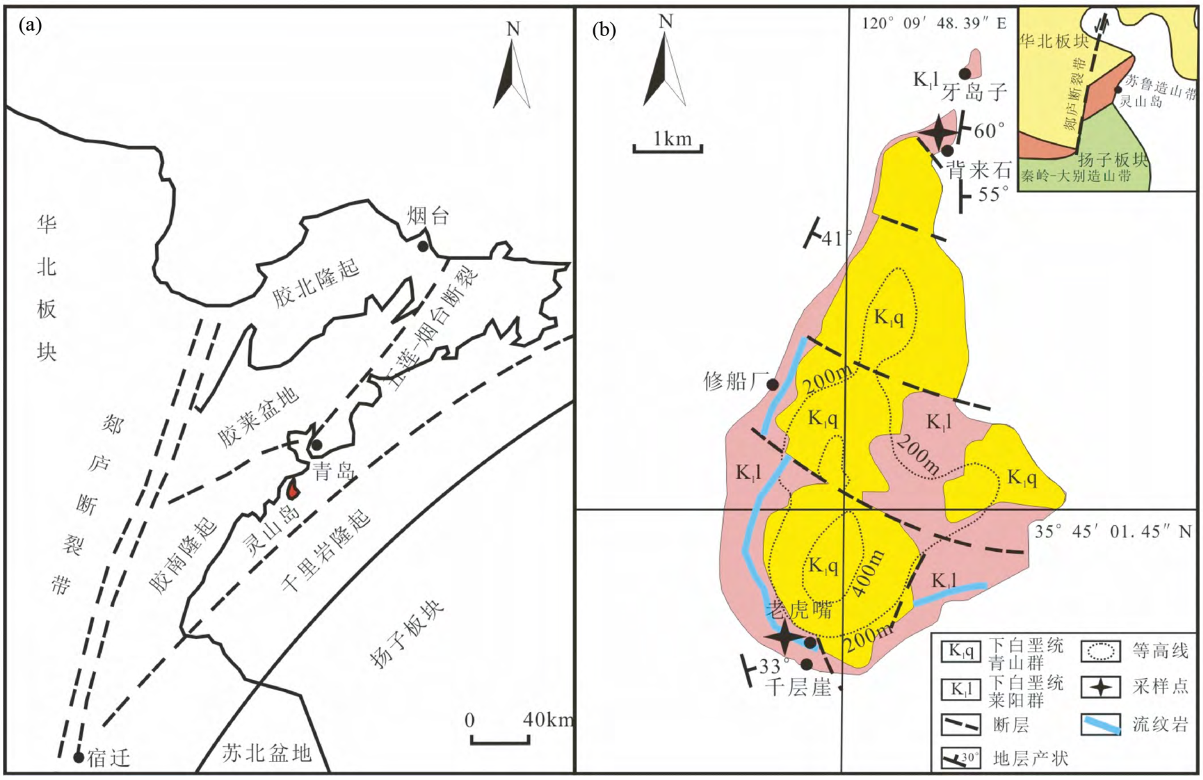

图1 灵山岛大地构造位置及其地质简图(据李杰等，2015；张振凯等，2017修改)

Fig. 1 The sketch map showing geotectonic position and geological framework of Lingshan Island (modified after Li *et al.*, 2015; Zhang *et al.*, 2017)

于华北地块，东南部胶南隆起带属于苏鲁造山带的北带(张岳桥，2006)。大量研究表明，区域上燕山期岩浆活动非常发育，构成中国东部中生代岩浆岩带的重要组成部分，并造成中国东部在中生代期间大规模构造格架转换和强烈大陆岩石圈减薄(Zhou and Lü，2000；张旗等，2001；翟明国和樊祺诚，2002；翟明国等，2004；Wu *et al.*，2005；邱连贵等，2008；Yang *et al.*，2008；朱日祥等，2011；Zhai and Santosh，2013；Liu *et al.*，2015；刘燊等，2016；Li *et al.*，2018)。

灵山岛地层和岩石组合大致可划分为5个单元(图2)(张海春等，2013；Wang *et al.*，2014)：①下部砂岩-粉砂岩、泥岩、碳质泥页岩沉积；②中部白色流纹岩、凝灰质流纹岩；③中上部含砾砂岩-粗砂岩、砾岩及磨拉石堆积；④上部火山凝灰岩、火山角砾岩和集块岩。⑤局部侵入碎屑沉积岩地层的基性岩墙(脉)。其中，底部的碎屑沉积岩大量发育不同尺度、不同类型的槽模、布丁状、球-枕状、火焰状等软沉积变形和同沉积构造，部分学者认为这套地层是一套地震诱发的深海静水浊积岩(吕洪波等，2011，2012)，也有学者认为是一套陆相三角洲浅水沉积或湖盆三角洲前缘沉积(钟建华，2012；邵珠福等，2014a，b；钟建华等，2016)。

关于地层形成时代方面，部分学者根据泥岩中的孢粉组合和砂岩中的碎屑锆石测年结果将灵山岛地层时代限定为晚侏罗世-早白垩世早期(吕洪波等，2011；张海春等，2013；Wang *et al.*，2014)。灵山岛海岸线大部分地区出露有流纹岩(图1b)，沿着南部千层崖剖面-西部造船厂剖面-东南部洋礁洞剖面山腰处均有出露，在北部背来石剖面处缺失，推测可能被剥蚀殆尽。老虎嘴和洋礁洞剖面的流纹岩最厚可达15～20m，其余地区出露的流纹岩最薄约1m厚，可作为全岛的标志层。已有学者对灵山岛白色流纹岩进行LA-ICP-MS锆石U-Pb测年分析，获得了119.2～123.9Ma的成岩年龄(Wang *et al.*，2014；周瑶琪等，2015b)，基本上把灵山岛地层的沉积年龄限定在了早白垩世(～120Ma)。关于灵山岛北端的陆相沉积砾岩-粗砂岩和灵山岛东部-南部的磨拉石堆积仅有零星研究(张星等，2012；董晓朋等，2014)。砾岩和磨拉石中含有大量片麻岩和石英岩砾石，标志着沉积盆地的变窄、变浅、接近物源区以及后期的快速隆升事件(董晓朋等，2014)。灵山岛火山角砾岩、集块岩等目前尚无相关研究报道。灵山岛多处发育基性岩墙或者岩脉(千层崖、背来石剖面等)。此外，胶东的其他多个地区(如日照、丁字湾、海洋采石场等)也大量发育有镁铁质-长英质中生代岩脉，镁铁质岩脉以煌斑岩、辉绿岩、辉长岩为主，少量长英质岩脉主要是闪长岩和二长岩等(周瑶琪等，2015b；刘菲菲等，2016)。这些岩脉的形成年龄主要集中于90～140Ma(Liu *et al.*，2004，2009)，呈NE-SW向展布。总体来看，灵山岛下部沉积地层可与胶莱盆地下白垩统莱阳群法家茔组(K_1f)对比，上

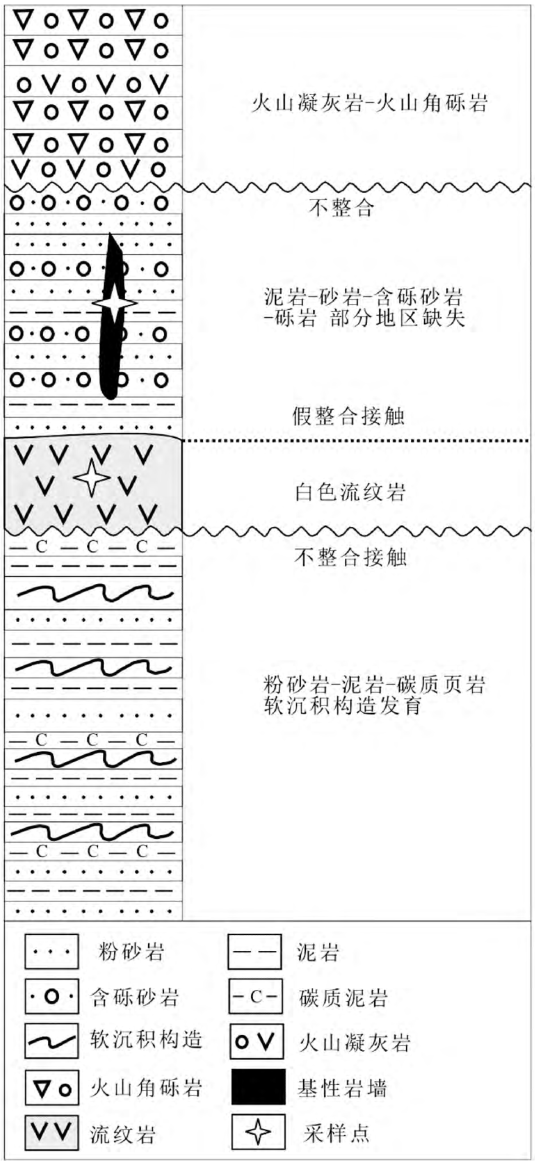

图2 灵山岛地层剖面示意图(据 Wang *et al.*，2014 修改)

Fig. 2 Lithostratigraphy of Lingshan Island (modified after Wang *et al.*，2014)

部火山-碎屑岩地层属于下白垩统青山群八亩地组(K_1b)(山东省第四地质矿产勘查院，2003; 栾光忠等，2010)。其中，莱阳群系一套陆相盆地(河、湖相)碎屑岩夹火山岩沉积，其上被早白垩世青山群不整合覆盖。而青山群为一套陆相火山岩-火山碎屑岩盆地沉积，在鲁东地区以中-酸性岩为主，呈面状大面积分布; 鲁西地区以中基性为主，呈小规模带状分布。青山群火山岩在鲁东和鲁西虽然横向岩性变化大，但同一层位时代大致相同，集中在 98 ~ 122Ma(邱检生等，2001，2012; 凌文黎等，2006; 唐嘉锋等，2008; Ling *et al.*，2009)。鲁东和鲁西地区沉积-岩浆构造演化格局揭示了古太平洋板块俯冲对欧亚板块的影响，为中国东部晚中生代构造体制转换和岩石圈减薄过程提供了重要的动力机制。

2 样品岩相学特征

本文选取灵山岛南部老虎嘴景区的白色流纹岩样品(LHZ)和灵山岛最北部背来石处的基性岩墙样品(BLS04)为研究对象，进行原位锆石 U-Pb-Hf 同位素分析和地球化学分析。

流纹岩覆盖于粉砂岩-泥岩-碳质页岩之上，局部角岩化。岩石露头新鲜，出露厚度约 15m，局部地区可观察到明显的流动构造，未变质变形(图 3a)。岩石具有斑状结构，斑晶主要为石英(~5%)和碱性长石(8% ~15%)，石英斑晶表面干净，呈大小不等的他形粒状，钾长石斑晶呈半自形-自形板柱状，表面多高岭土化和绢云母化; 基质为微晶-隐晶质结构，成分主要是石英和长石，含量 80% ~85%(图 3d)，副矿物包括锆石、磷灰石、金红石和磁铁矿。通过岩石学和岩相学观察、对比，推测流纹岩与下伏地层之间为不整合接触关系。主要原因是野外观测到流纹岩层与下伏沉积岩层之间呈波浪状起伏不平，并且下部沉积岩层顶部偶尔可见剥蚀痕迹。除此之外，下部的粉砂岩-泥岩-碳质页岩地层大量发育滑塌褶皱和软沉积变形(吕洪波等，2011，2012)，是典型的水下沉积构造。而上部的流纹岩中并未观察到典型的水下快速冷凝结构，如: 联斑晶、淬火和裂纹结构(富公勤和李树钧，1987)。因此，上部和下部岩石不同的产出环境也揭示二者间存在一不整合间断，代表一次小规模隆升。

灵山岛北部基性岩墙近垂直地侵入陆相泥岩-粗砂岩-含砾砂岩碎屑沉积岩层，岩墙张性节理发育，表面风化呈灰褐色，新鲜面为绿灰色，宽约 20cm，沿北东-南西走向(230°)发育(图 3b，c)。由于基性岩墙产出于灵山岛北部背来石地区，而该地区流纹岩缺失。因此，野外并未观察到二者的直接接触关系。岩石显示斑状结构，斑晶为半自形-他形单斜辉石(~5%)和斜长石(5% ~7%)，斑晶粒度最大可达 1 ~3mm。大部分单斜辉石斑晶边部蚀变为绿泥石，部分单斜辉石彻底蚀变为绿泥石(表 1)，斜长石斑晶受热液交代作用发生碳酸盐化(图 3e-h); 基质(80% ~85%)呈板条-架状结构，主要由长石雏晶、角闪石、辉石及其蚀变矿物黑云母等组成(图 3e，f); 副矿物包括锆石和磁铁矿(图 3h)。绿泥石、碳酸盐矿物和石英的出现指示岩石经历了后期热液交代。结合野外产状和显微镜下矿物结构，该岩墙属于次火山相超浅成辉绿玢岩岩墙，是在接近地表情况下结晶冷凝形成的侵入岩-火山岩过渡相。此外，辉绿玢岩岩墙展布方向与鲁东地区广泛发育的岩墙展布方向(NE-SW)近乎一致(Guo *et al.*，2004; Liu *et al.*，2004，2009; Ma *et al.*，2014)，表明在区域拉张背景下形成了一系列裂隙通道，而后岩浆沿通道灌入形成岩墙。

表1 灵山岛辉绿玢岩样品中单斜辉石及其边部蚀变绿泥石矿物化学成分(wt%)

Table 1 Major element compositions of clinopyroxene and chlorite on its rim in diabase porphyrite from the Lingshan Island (wt%)

测点号	bls04-1	bls04-2	bls04-3	bls04-4	bls04-1	bls04-2	bls04-3	bls04-4
	Cpx				Chl			
K_2O	0.01	0.00	0.00	0.00	0.00	0.03	0.02	0.05
CaO	22.53	22.48	22.11	22.42	0.21	0.20	0.13	0.30
TiO_2	1.17	1.42	1.12	0.81	0.00	0.02	0.00	0.03
Na_2O	0.23	0.24	0.21	0.17	0.01	0.03	0.04	0.06
Al_2O_3	4.38	5.00	4.37	2.82	13.17	13.55	16.24	12.75
MgO	14.43	13.65	14.25	15.41	19.89	21.11	20.73	20.36
SiO_2	49.44	48.79	49.62	51.31	30.78	32.49	31.18	31.34
FeO^T	5.85	6.42	5.92	5.57	18.26	17.50	17.84	17.10
MnO	0.14	0.12	0.04	0.08	0.12	0.12	0.09	0.05
Cr_2O_3	0.48	0.21	0.55	0.37	0.54	0.47	0.65	0.38
Total	98.64	98.33	98.18	98.95	82.98	85.51	86.92	82.41

注:测试在西北大学大陆动力学国家重点实验室完成,应用日本电子(JEOL)公司生产的JXA-8230型电子探针进行分析,电子束加速电压为15kV,电子束电流为10nA,电子束直径采用2μm

3 样品分析方法

锆石分选工作在河北省廊坊市区调研究所实验室完成,全岩主、微量元素(包括稀土元素)分析、锆石制靶和CL图像照射、锆石U-Pb定年和Lu-Hf同位素测定均在西北大学大陆动力学国家重点实验室完成。

全岩主量元素分析采用玻璃熔饼法在X荧光光谱仪(XRF, Rigaku RIX2100)上测定,分析精度优于2%;全岩微量和稀土元素测试在电感耦合等离子质谱(ICP-MS)仪上测定,样品测试过程中以AGV-2、BHVO-2、BCR-2、GSP-1为标样监控,分析误差小于5%~10%(刘晔等,2007)。

锆石U-Pb年龄测定之前,将人工重砂分离出的锆石颗粒随机固定在环氧树脂表面并抛光,进行透射光、反射光和阴极发光(CL)照相,以选定最佳测定部位。锆石U-Pb年龄和微量元素分析是在连接193nm深紫外ArF激光器(Geolas 2005)的Agilent 7500型ICP-MS上进行的,激光束斑直径为32μm,采用单点剥蚀方式,激光剥蚀样品深度为20~30μm。数据处理采用Glitter(Ver4.0)程序,年龄计算选取标准锆石91500为外标进行同位素比值分馏校正,元素浓度计算采用NIST610做外标,^{29}Si为内标,样品的锆石U-Pb年龄谐和图、加权平均年龄计算及图件绘制应用Isoplot软件(Ludwig, 2003)。

锆石原位Lu-Hf同位素分析的激光剥蚀系统是193nm准分子激光剥蚀系统(RESOlution M-50, ASI),包含一台193nm ArF准分子激光器,一个双室样品室和电脑控制的高精度X-Y样品台移动、定位系统。双室样品池能有效避免样品间交叉污染,减少样品吹扫时间,同时装载样品能力大大提高,减少了频繁换样过程中人为因素的影响。激光能量密度为6J/cm²,频率为5Hz,斑束为44μm,载气为高纯氦气,为280mL/min。Lu-Hf同位素分析采用多接收等离子体质谱(Nu Plasma Ⅱ MC-ICPMS),该设备是Nu Instrument公司的最新一代双聚焦多接收等离子体质谱仪。Lu-Hf同位素分馏校正采用指数法则计算,用$^{176}Lu/^{175}Lu=0.02656$(Blichert-Toft *et al.*, 1997)和$^{176}Yb/^{173}Yb=0.78696$(Thirlwall and Anczkiewicz, 2004)比值扣除^{176}Lu和^{176}Yb对^{176}Hf的干扰,获得准确的^{176}Hf信号值。Hf和Lu同位素比值采用$^{179}Hf/^{177}Hf=0.7325$(Patchett and Tatsumoto, 1981)进行仪器质量歧视效应校正,Yb同位素比值采用$^{173}Yb/^{171}Yb=1.12346$(Thirlwall and Anczkiewicz, 2004)进行仪器质量歧视效应校正。在分析过程中,国际标准锆石样品91500和Mud Tank作为监控样品,详细的仪器参数和分析方法见(Yuan *et al.*, 2008; Bao *et al.*, 2017)。$\varepsilon_{Hf}(t)$值计算采用的^{176}Lu衰变常数为$1.867\times10^{-11}y^{-1}$(Albarède *et al.*, 2006),球粒陨石的$^{176}Hf/^{177}Hf$比值为0.282785,$^{176}Lu/^{177}Hf$的比值为0.0336(Bouvier *et al.*, 2008)。Hf单阶段模式年龄t_{DM}的计算以现今的亏损地幔值为参考,其$^{176}Hf/^{177}Hf=0.28325$,$^{176}Lu/^{177}Hf=0.0384$(Griffin *et al.*, 2000)。两阶段Hf模式年龄(t_{DM2})计算时,平均地壳的值采用$^{176}Lu/^{177}Hf=0.015$(Rudnick and Gao, 2003)。

4 分析结果

4.1 岩石化学分析结果

4.1.1 主量元素组成

灵山岛流纹岩和辉绿玢岩样品的主、微量元素分析结果见表2。

主量元素分析结果显示,流纹岩样品的烧失量(LOI)介于0.82%~1.07%之间(表2),表明流纹岩未遭受过蚀变或变质影响。该流纹岩具有高硅(SiO_2=75.13%~75.82%)、

表 2　灵山岛流纹岩和辉绿玢岩样品主量元素(wt%)和微量元素($\times 10^{-6}$)分析结果

Table 2　Major (wt%) and trace element ($\times 10^{-6}$) for rhyolite and diabase porphyrite from the Lingshan Island

样品号	LHZ01	LHZ02	LHZ03	LHZ04	LHZ05	LHZ06	LHZ07	LHZ08	LHZ09	LHZ10	BLS-04-1	BLS-04-2	BLS-04-3	BLS-04-4	BLS-04-5	BLS-04-6	BLS-04-7	BLS-04-8	BLS-04-9	BLS-04-10
岩性	流纹岩										辉绿玢岩									
SiO_2	75.46	75.24	75.82	75.58	75.31	75.74	75.41	75.45	75.47	75.13	51.60	51.93	51.73	51.83	51.97	51.53	51.17	51.92	51.59	51.24
TiO_2	0.08	0.08	0.08	0.09	0.08	0.08	0.09	0.09	0.09	0.09	1.69	1.69	1.68	1.62	1.63	1.69	1.75	1.67	1.71	1.72
Al_2O_3	13.18	13.15	13.21	13.20	13.17	13.17	13.24	13.23	13.20	13.15	15.11	15.16	14.68	13.80	14.13	15.15	15.44	14.45	14.93	15.19
$Fe_2O_3^T$	0.80	0.83	0.80	0.81	0.79	0.82	0.79	0.81	0.83	0.81	9.14	8.97	9.22	9.60	9.48	9.05	9.47	9.48	9.34	9.23
MnO	0.06	0.05	0.06	0.06	0.06	0.06	0.06	0.06	0.06	0.05	0.13	0.12	0.13	0.13	0.13	0.13	0.12	0.13	0.13	0.13
MgO	0.15	0.13	0.14	0.14	0.12	0.14	0.14	0.14	0.13	0.14	8.40	8.10	8.66	9.34	9.07	8.10	9.00	9.02	8.64	8.48
CaO	0.19	0.46	0.11	0.10	0.33	0.10	0.30	0.37	0.22	0.31	7.28	7.33	7.45	7.97	7.61	7.52	6.49	7.26	7.14	7.31
Na_2O	4.61	4.73	4.65	4.63	4.68	4.58	4.71	4.87	4.68	4.74	2.64	2.69	2.60	2.28	2.38	2.75	2.48	2.37	2.59	2.66
K_2O	4.38	4.10	4.34	4.42	4.29	4.37	4.22	4.19	4.20	4.19	3.24	3.26	3.10	2.73	2.90	3.32	3.31	2.97	3.19	3.27
P_2O_5	0.07	0.15	0.02	0.01	0.01	0.01	0.01	0.01	0.01	0.01	0.76	0.75	0.74	0.70	0.71	0.76	0.77	0.73	0.74	0.76
LOI	0.86	0.99	0.82	0.93	1.07	0.92	0.99	1.01	0.94	1.05	6.48	6.70	6.62	7.32	6.69	6.13	7.55	7.05	6.56	6.64
Total	99.84	99.91	100.05	99.97	99.91	99.99	99.96	100.23	99.83	99.67	99.88	99.75	100.12	99.92	99.88	99.53	99.53	99.97	99.68	99.55
A/CNK	1.04	1.01	1.05	1.05	1.02	1.06	1.03	1.00	1.04	1.02	0.72	0.71	0.69	0.65	0.68	0.70	0.79	0.71	0.72	0.72
$Mg^{\#}$	30.4	26.7	29.0	28.7	26.1	28.5	29.2	28.7	26.7	28.7	68.2	67.8	68.7	69.4	69.0	67.6	68.9	68.9	68.3	68.2
σ	2.49	2.42	2.46	2.51	2.49	2.45	2.46	2.53	2.43	2.48	4.03	3.96	3.72	2.85	3.11	4.32	4.09	3.20	3.89	4.27
K_2O+Na_2O	8.99	8.83	8.99	9.05	8.97	8.95	8.93	9.06	8.88	8.93	5.89	5.94	5.70	5.01	5.28	6.07	5.78	5.34	5.78	5.93
K_2O/Na_2O	0.63	0.57	0.61	0.63	0.60	0.63	0.59	0.57	0.59	0.58	0.81	0.80	0.79	0.79	0.80	0.79	0.88	0.83	0.81	0.81
Li	2.66	2.91	2.72	2.79	2.85	2.80	2.94	2.81	2.84	2.77	66.6	64.0	62.6	70.0	68.4	58.7	78.7	72.2	66.9	67.0
Be	2.67	3.21	2.64	2.65	3.56	2.75	3.91	3.51	3.66	3.50	2.26	2.21	2.03	2.12	2.10	2.11	2.35	2.23	2.21	2.25
Sc	2.59	2.45	2.53	2.55	2.60	2.58	2.52	2.56	2.51	2.53	23.0	22.9	24.3	26.0	25.4	22.9	23.5	24.2	23.7	22.8
V	0.92	0.89	0.74	0.79	0.84	0.75	0.82	0.83	0.82	0.82	180	181	182	178	178	182	177	178	182	180
Cr	1.53	5.95	2.00	0.93	1.36	1.10	0.89	2.55	1.82	1.17	396	423	425	578	492	370	406	466	399	384
Co	39.4	23.0	28.2	37.9	29.5	36.2	28.2	30.6	31.7	31.0	44.1	45.1	43.3	48.5	45.7	44.0	42.1	44.4	43.2	43.7
Ni	1.64	4.42	1.62	1.23	1.48	1.40	1.09	2.30	2.23	1.31	181	192	182	252	211	167	182	201	179	177
Cu	0.61	0.73	0.58	0.94	0.57	0.49	0.71	0.57	0.53	0.73	47.2	46.8	45.8	45.8	45.6	46.0	48.0	45.4	46.6	46.9
Zn	29.8	28.0	23.5	28.0	30.1	36.3	27.3	28.1	27.3	27.4	83.4	85.7	84.5	88.0	80.7	82.2	85.1	78.7	78.3	83.5
Ga	18.2	18.4	18.2	18.6	18.3	18.3	18.4	18.3	18.4	18.5	17.8	18.0	17.4	16.4	16.9	17.7	18.3	17.2	17.8	18.0
Ge	0.95	0.95	0.93	0.97	0.93	0.95	0.95	0.92	0.93	0.95	1.32	1.33	1.32	1.35	1.36	1.33	1.37	1.33	1.33	1.33
Rb	84.7	77.9	83.7	87.0	82.8	85.1	80.5	80.0	80.0	80.1	71.2	71.7	66.4	58.9	62.6	71.3	72.5	64.8	69.3	71.1
Sr	117	123	115	117	125	114	122	123	121	122	611	616	597	573	589	638	545	576	604	590

续表 2

Continued Table 2

样品号	LHZ01	LHZ02	LHZ03	LHZ04	LHZ05	LHZ06	LHZ07	LHZ08	LHZ09	LHZ10	BLS-04-1	BLS-04-2	BLS-04-3	BLS-04-4	BLS-04-5	BLS-04-6	BLS-04-7	BLS-04-8	BLS-04-9	BLS-04-10
岩性	流纹岩										辉绿玢岩									
Y	23.4	22.3	22.7	23.8	23.3	23.1	23.3	23.1	23.2	23.0	22.7	22.5	21.9	20.9	21.2	22.4	23.9	21.3	22.6	22.6
Zr	123	120	126	127	130	126	125	123	124	123	203	204	197	186	191	204	204	194	203	203
Nb	17.4	17.6	17.1	18.0	18.0	18.0	18.1	18.0	18.3	18.3	33.5	34.3	32.7	30.2	31.6	33.7	33.9	32.0	33.6	33.8
Cs	0.23	0.22	0.22	0.23	0.23	0.22	0.22	0.23	0.22	0.22	0.87	0.92	0.88	0.94	0.90	0.82	1.07	0.92	0.90	0.92
Ba	239	241	234	245	263	241	244	246	245	244	1866	1863	1780	1599	1715	1908	1775	1714	1855	1820
La	26.4	21.4	26.5	27.1	23.1	24.1	25.5	22.0	23.2	23.0	33.4	33.5	32.3	31.5	31.7	33.3	34.3	31.8	32.6	33.9
Ce	50.4	46.2	50.8	52.4	51.3	47.4	55.7	48.3	50.7	50.0	69.5	69.7	67.1	65.4	65.7	68.7	70.3	65.4	68.1	69.9
Pr	6.34	5.28	6.34	6.52	5.87	5.86	6.32	5.53	5.80	5.73	8.51	8.56	8.20	7.96	7.98	8.43	8.57	7.94	8.28	8.56
Nd	21.7	18.2	21.7	22.4	20.2	20.1	21.7	19.1	20.0	19.7	34.3	34.5	33.2	32.0	32.3	34.1	34.6	32.0	33.5	34.8
Sm	4.63	4.00	4.55	4.73	4.42	4.34	4.68	4.15	4.35	4.26	6.50	6.52	6.30	6.09	6.17	6.48	6.54	6.00	6.36	6.50
Eu	0.39	0.34	0.38	0.40	0.37	0.36	0.40	0.35	0.37	0.37	2.32	2.34	2.20	2.13	2.14	2.33	2.36	2.08	2.23	2.36
Gd	4.02	3.57	3.94	4.14	3.86	3.82	4.03	3.67	3.80	3.75	5.73	5.77	5.53	5.38	5.35	5.70	5.76	5.39	5.65	5.80
Tb	0.64	0.59	0.62	0.64	0.62	0.61	0.63	0.60	0.61	0.61	0.78	0.78	0.75	0.73	0.73	0.77	0.79	0.73	0.77	0.77
Dy	3.82	3.64	3.75	3.89	3.79	3.71	3.83	3.72	3.72	3.70	4.30	4.37	4.22	4.05	4.15	4.31	4.49	4.13	4.33	4.37
Ho	0.77	0.74	0.75	0.78	0.76	0.75	0.76	0.75	0.76	0.75	0.82	0.83	0.80	0.77	0.78	0.81	0.85	0.78	0.82	0.81
Er	2.27	2.21	2.21	2.32	2.28	2.25	2.25	2.25	2.25	2.22	2.24	2.26	2.19	2.12	2.13	2.22	2.32	2.15	2.25	2.24
Tm	0.34	0.33	0.33	0.35	0.34	0.34	0.34	0.34	0.34	0.33	0.31	0.31	0.30	0.29	0.30	0.31	0.32	0.30	0.31	0.31
Yb	2.26	2.24	2.21	2.30	2.30	2.29	2.25	2.27	2.26	2.25	1.99	1.97	1.92	1.84	1.87	1.98	2.04	1.89	1.98	1.98
Lu	0.33	0.33	0.33	0.34	0.34	0.34	0.33	0.33	0.33	0.33	0.29	0.29	0.28	0.27	0.27	0.29	0.30	0.28	0.29	0.29
Hf	4.94	4.87	5.00	5.06	5.11	4.97	4.96	4.92	4.92	4.87	4.94	4.97	4.82	4.54	4.64	4.93	4.96	4.72	4.94	4.92
Ta	1.20	1.16	1.17	1.21	1.20	1.18	1.17	1.15	1.18	1.17	1.96	1.99	1.89	1.75	1.80	1.95	1.97	1.85	1.94	1.97
Pb	23.4	26.8	21.9	27.4	26.2	24.5	28.9	29.6	26.3	26.2	7.34	7.60	7.26	6.33	6.45	7.19	8.43	6.71	6.47	8.23
Th	10.5	10.3	10.3	10.6	10.6	10.3	10.3	10.3	10.3	10.3	3.02	3.05	2.89	2.66	2.76	2.98	3.00	2.81	2.97	2.98
U	1.47	1.43	1.39	1.45	1.47	1.43	1.40	1.40	1.38	1.38	0.90	0.91	0.87	0.80	0.82	0.89	0.93	0.85	0.89	0.90
∑REE	124.3	109.0	124.3	128.3	119.6	116.3	128.8	113.4	118.4	117.1	170.9	171.7	165.2	160.6	161.5	169.8	173.5	160.9	167.5	172.6
LREE	109.8	95.36	110.2	113.5	105.3	102.1	114.3	99.43	104.4	103.1	154.5	155.2	149.2	145.2	145.9	153.4	156.6	145.3	151.1	156.0
HREE	14.45	13.66	14.14	14.76	14.29	14.11	14.43	13.94	14.07	13.95	16.45	16.57	16.00	15.44	15.58	16.39	16.86	15.64	16.40	16.58
LREE/HREE	7.60	6.98	7.79	7.69	7.37	7.24	7.92	7.13	7.42	7.39	9.39	9.37	9.33	9.40	9.37	9.36	9.29	9.29	9.21	9.41
δEu	0.27	0.27	0.28	0.27	0.27	0.27	0.28	0.27	0.28	0.28	1.16	1.17	1.14	1.14	1.14	1.17	1.18	1.12	1.14	1.18
$(La/Yb)_N$	7.88	6.42	8.09	7.95	6.76	7.10	7.63	6.53	6.93	6.89	11.3	11.5	11.3	11.6	11.4	11.3	11.4	11.3	11.1	11.6

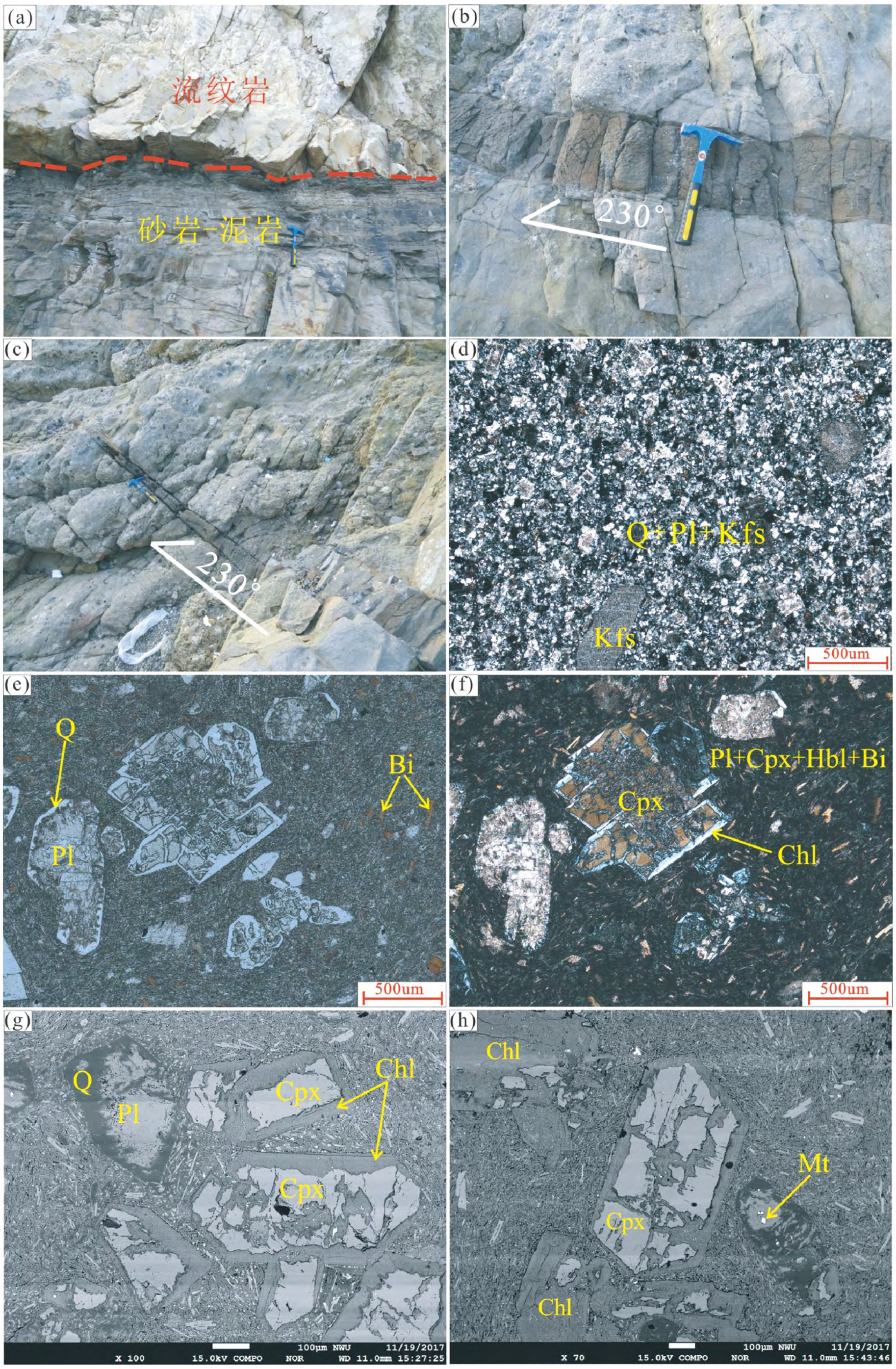

图 3　灵山岛白色流纹岩和辉绿玢岩特征

(a) 流纹岩不整合覆盖于碎屑岩之上;(b、c) 辉绿玢岩侵入砂岩地层;(d) 流纹岩正交偏光下特征;辉绿玢岩单偏光下(e) 和正交偏光下(f) 特征;(g、h) 辉绿玢岩背散射照片 . Pl-斜长石;Q-石英;Cpx-单斜辉石;Bi-黑云母;Hbl-角闪石;Mt-磁铁矿;Chl-绿泥石;Kfs-钾长石

Fig. 3　The characteristics of rhyolite and diabase porphyrite dyke in the Lingshan Island

(a) rhyolite unconformably covers clastic strata; (b, c) diabase porphyrite intrudes the clastic strata; (d) cross-polarized light microphotographs of rhyolite; plane polarized light (e) and cross-polarized light (f) microphotographs of diabase porphyrite dyke; (g, h) backscattered electron (BSE) images of diabase porphyrite dyke. Pl-plagioclase; Q-quartz; Cpx-clinopyroxene; Bi-biotite; Hb-hornblende; Mt-magnetite; Chl-chlorite; Kfs-potash feldspar

富钾(K_2O = 4.10% ~ 4.42%)、富碱($K_2O + Na_2O$ = 8.83% ~ 9.06%),贫钙(CaO = 0.10% ~ 0.46%)、富铝(Al_2O_3 = 13.15% ~ 13.24%),低铁($Fe_2O_3^T$ = 0.79% ~ 0.83%)、低镁(MgO = 0.12% ~ 0.15%)和低钛(TiO_2 = 0.08% ~ 0.09%)的特征,K_2O/Na_2O = 0.57 ~ 0.63,$Mg^{\#}$ = 26.1 ~ 30.4(表 2)。A/CNK = 1.00 ~ 1.06,属于弱过铝质岩石。在 TAS 判别图解

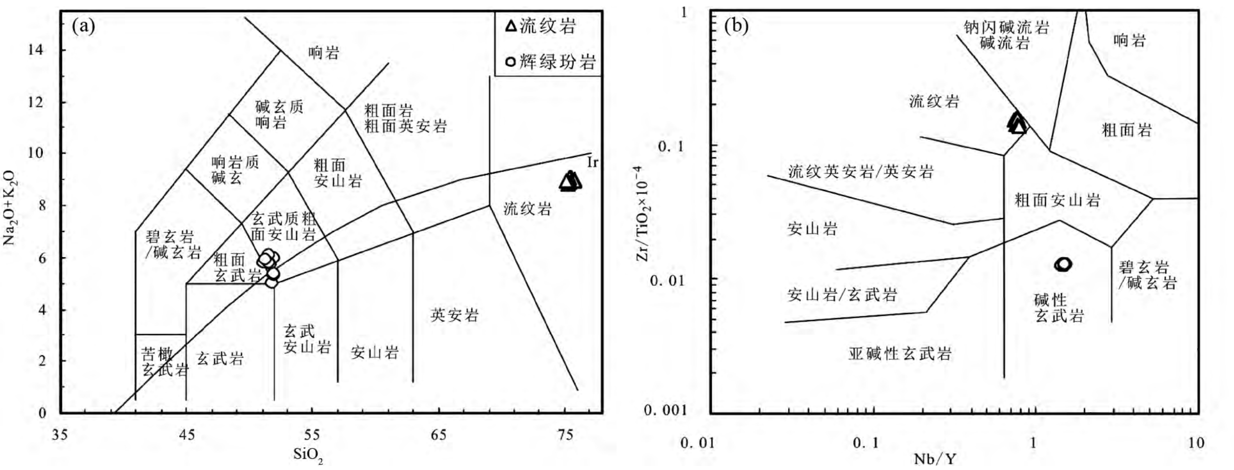

图4 灵山岛流纹岩和辉绿玢岩 TAS (a) 和 $Nb/Y-Zr/TiO_2 \times 10^{-4}$ (b) 岩石类型判别图解(据 Le Bas *et al.*, 1986; Irvine and Baragar, 1971; Winchester and Floyd, 1977)

Fig. 4 Diagrams of total alkali vs. SiO_2 (a) and Nb/Y vs. $Zr/TiO_2 \times 10^{-4}$ (b) for the rhyolite and diabase porphyrite dyke from Lingshan Island (after Le Bas *et al.*, 1986; Irvine and Baragar, 1971; Winchester and Floyd, 1977)

和 $Nb/Y-Zr/TiO_2 \times 10^{-4}$ 图解中,所有分析样品均落入亚碱性流纹岩区域(图4);在 A/CNK-A/NK 图解中,样品落入弱过铝质岩石系列(图5a);在 K_2O-SiO_2 图解中,样品显示为高钾钙碱性岩石系列(图5b)。

辉绿玢岩样品具有相对较高的烧失量(LOI = 6.13% ~ 7.55%),可能与样品中辉石蚀变为云母、绿泥石等含水矿物以及岩石碳酸盐化相关。故表2列出的数据是在扣除烧失量并换算成100%后的值。该辉绿玢岩样品的 SiO_2 含量为 51.17% ~ 51.97%,Al_2O_3 含量为 13.80% ~ 15.44%,平均值 14.80%,CaO = 6.49% ~ 7.97%,K_2O = 2.90% ~ 3.32%,全碱 $K_2O + Na_2O$ = 5.01% ~ 6.07%,K_2O/Na_2O = 0.79 ~ 0.88,MgO = 8.10% ~ 9.34%,全铁 $Fe_2O_3^T$ = 8.97% ~ 9.60%,TiO_2 含量为 1.62% ~ 1.75%,$Mg^\#$ 值较高,约为 67.6 ~ 69.4。里特曼指数 σ = 2.85 ~ 4.32,属于偏碱性岩石系列。在 TAS 判别图解和 $Nb/Y-Zr/TiO_2 \times 10^{-4}$ 岩石类型划分图解中,所有辉绿玢岩分析样品落在粗面玄武岩-玄武质粗面安山岩(图4a)和碱性玄武岩(图4b)区域;在 K_2O-SiO_2 图解中,样品显示属于钾玄岩岩石系列(图5b)。

4.1.2 微量元素组成

灵山岛流纹岩样品稀土总量较低($\sum REE = 109.0 \times 10^{-6} \sim 128.8 \times 10^{-6}$)。轻、重稀土元素分异较弱,$(La/Yb)_N$ = 6.42 ~ 8.09;轻稀土元素相对富集,重稀土元素相对轻微亏损,LREE/HREE = 6.98 ~ 7.92。Eu 和 Sr 具有明显负异常特征,δEu = 0.27 ~ 0.28,暗示斜长石的结晶分异作用。Cr、Ni 含量低且变化较大,$Cr = 0.89 \times 10^{-6} \sim 5.95 \times 10^{-6}$; $Ni = 1.09 \times 10^{-6} \sim 4.42 \times 10^{-6}$。在球粒陨石标准化稀土元素配分曲线上(图6a),样品显示右倾平坦型分布模式,具有上地壳稀土元素的特征。原始地幔标准化微量元素蛛网图显示(图6b),大离子亲石元素 Rb、Th 和 Pb 相对富集,高场强元素 Nb 和 Ta 轻微负异常,Ti 明显负异常,说明源区部分熔融残留相并非金红石,或者岩浆演化过程没有金红石的结晶分异。

辉绿玢岩样品稀土元素含量较高($\sum REE = 160.6 \times 10^{-6} \sim 173.5 \times 10^{-6}$),轻、重稀土元素分异明显,$(La/Yb)_N$ = 11.1 ~ 11.6;轻稀土元素相对富集,重稀土元素相对亏损,LREE/HREE = 9.21 ~ 9.41。轻微 Eu 正异常(δEu = 1.12 ~ 1.18),指示岩浆演化过程中无斜长石结晶分异。稀土元素球粒陨石标准化配分曲线显示,样品具有右倾平坦的 REE 配分模式,与洋岛玄武岩(OIB)的稀土配分曲线类似(图6c; Sun and McDonough, 1989)。微量元素原始地幔标准化蛛网图显示(图6d),样品相对富集 Rb、Ba 和 Pb,虽然样品高场强元素 Nb、Ta 无明显异常,Ti 轻微负异常,但是具有相对富集的 Rb、Ba 和 Pb,指示地壳物质的贡献,岩浆可能起源于富集地幔源区或有轻微地壳混染。亲铁元素 Cr($370 \times 10^{-6} \sim 578 \times 10^{-6}$)和 Ni($167 \times 10^{-6} \sim 252 \times 10^{-6}$)含量较高。这些特征与板内碱性玄武岩基本一致。

4.2 LA-ICP-MS 锆石 U-Pb 年龄

白色流纹岩样品(LHZ)中的锆石无色、透明,呈半自形-自形长柱状,长轴粒径介于 100 ~ 160μm,长宽比为 1∶1 ~ 3∶1(图7a)。CL 图像显示锆石发光性好,具有明显的岩浆振荡环带(图7a)。锆石的 Th、U 含量分别为 $25.7 \times 10^{-6} \sim 5545 \times 10^{-6}$ 和 $46.5 \times 10^{-6} \sim 2221 \times 10^{-6}$,Th/U 比值为 0.44 ~ 2.99,平均 1.64(表3),显示典型的岩浆成因锆石特点(Hoskin and Black, 2000; Belousova *et al.*, 2002; Hoskin and Schaltegger, 2003)。随机选取样品(LHZ)中 30 个锆石测点进行 LA-ICP-MS U-Pb 年龄分析。剔除 4 个不谐和年龄,其余有 4 颗锆石核部的 $^{206}Pb/^{238}U$ 年龄为 702 ~ 730Ma 左右,

表 3 灵山岛流纹岩和辉绿玢岩 LA-ICP-MS 锆石 U-Pb 定年结果

Table 3 LA-ICP-MS zircon U-Pb dating results for rhyolite and diabase porphyrite from the Lingshan Island

测点号	含量($\times 10^{-6}$)			Th/U	同位素比值						年龄(Ma)					
	Pb*	Th	U		$\frac{^{206}Pb}{^{238}U}$	2σ	$\frac{^{207}Pb}{^{235}U}$	2σ	$\frac{^{207}Pb}{^{206}Pb}$	2σ	$\frac{^{206}Pb}{^{238}U}$	2σ	$\frac{^{207}Pb}{^{235}U}$	2σ	$\frac{^{207}Pb}{^{206}Pb}$	2σ
LHZ 流纹岩																
LHZ-1	7.53	39.2	46.5	0.84	0.11990	0.00355	1.11507	0.13372	0.06734	0.00819	730	20	761	64	848	234
LHZ-2	15.9	1015	510	1.99	0.01761	0.00039	0.13927	0.01080	0.05725	0.00453	113	2	132	10	501	166
LHZ-3	3.88	158	149	1.06	0.01831	0.00063	0.13129	0.03310	0.05193	0.01319	117	4	125	30	282	496
LHZ-4	14.5	61.5	92.4	0.67	0.11964	0.00274	1.13965	0.07384	0.06898	0.00457	729	16	772	35	898	131
LHZ-5	4.19	274	134	2.04	0.01800	0.00072	0.13897	0.04033	0.05592	0.01635	115	5	132	36	449	545
LHZ-6	1.80	119	58.8	2.02	0.01714	0.00103	0.14486	0.09650	0.06122	0.04093	110	7	137	86	647	1017
LHZ-7	30.6	1722	1027	1.68	0.01779	0.00035	0.14643	0.00654	0.05962	0.00275	114	2	139	6	590	97
LHZ-8	10.8	876	293	2.99	0.01777	0.00048	0.12904	0.01953	0.05261	0.00804	114	3	123	18	312	315
LHZ-9	33.6	82.8	71.2	1.16	0.31537	0.00685	5.43937	0.18518	0.12494	0.00442	1767	34	1891	29	2028	61
LHZ-10	35.3	78.4	76.8	1.02	0.31716	0.00658	5.41990	0.16649	0.12380	0.00397	1776	32	1888	26	2012	56
LHZ-11	35.1	1947	1168	1.67	0.01840	0.00036	0.13758	0.00601	0.05417	0.00244	118	2	131	5	378	98
LHZ-12	6.69	290	239	1.21	0.01885	0.00053	0.13423	0.02315	0.05162	0.00898	120	3	128	21	269	356
LHZ-13	7.19	332	250	1.33	0.01891	0.00049	0.12996	0.02172	0.04981	0.00838	121	3	124	20	186	350
LHZ-15	6.22	274	216	1.27	0.01899	0.00057	0.13460	0.03888	0.05139	0.01490	121	4	128	35	258	557
LHZ-17	12.2	672	406	1.66	0.01908	0.00057	0.13475	0.02101	0.05123	0.00808	122	4	128	19	251	327
LHZ-18	83.8	5545	2221	2.50	0.01868	0.00037	0.14028	0.00559	0.05449	0.00224	119	2	133	5	391	89
LHZ-19	2.49	160	71.0	2.26	0.01836	0.00137	0.14437	0.12755	0.05707	0.05059	117	9	137	113	494	1267
LHZ-20	60.8	141	228	0.62	0.11966	0.00288	1.10268	0.06710	0.06689	0.00418	729	17	755	32	834	125
LHZ-21	15.6	991	478	2.08	0.01956	0.00066	0.13640	0.02363	0.05064	0.00889	125	4	130	21	225	362
LHZ-22	60.9	3737	1640	2.28	0.01908	0.00039	0.13832	0.00644	0.05267	0.00252	122	2	132	6	315	105
LHZ-23	8.57	25.7	58.6	0.44	0.11496	0.00375	1.07907	0.13686	0.06821	0.00879	702	22	743	67	875	246
LHZ-25	23.1	1438	660	2.18	0.01948	0.00053	0.13357	0.01535	0.04984	0.00582	124	3	127	14	187	251
LHZ-26	2.90	181	94.1	1.92	0.01864	0.00094	0.12686	0.05829	0.04951	0.02286	119	6	121	53	172	824
LHZ-27	3.32	191	104	1.83	0.01850	0.00137	0.13865	0.09310	0.05452	0.03681	118	9	132	83	392	1061
LHZ-29	7.76	406	279	1.46	0.01830	0.00059	0.13350	0.02373	0.05310	0.00954	117	4	127	21	333	363
LHZ-30	1.87	123	52.3	2.36	0.01952	0.00132	0.13257	0.11455	0.04944	0.04283	125	8	126	103	169	1304
BLS04 辉绿玢岩																
BLS04-01	14.7	297	584	0.51	0.01701	0.00038	0.11268	0.01136	0.04804	0.00491	109	2	108	10	101	225
BLS04-02	9.01	74.6	93.4	0.80	0.06994	0.00223	0.54765	0.08380	0.05679	0.00880	436	13	444	55	483	311
BLS04-03	157	89.5	364	0.25	0.28153	0.00510	5.79209	0.11354	0.14918	0.00324	1599	26	1945	17	2337	37
BLS04-04	141	139	335	0.41	0.32071	0.00578	6.70527	0.12816	0.15158	0.00322	1793	28	2073	17	2364	36
BLS04-05	22.8	61.3	53.1	1.16	0.29745	0.00684	5.00579	0.21932	0.12199	0.00552	1679	34	1820	37	1986	78
BLS04-06	75.0	180	152	1.18	0.32829	0.00686	5.68348	0.17541	0.12548	0.00407	1830	33	1929	27	2036	56
BLS04-07	46.0	156	77.1	2.03	0.33744	0.00713	5.81663	0.18886	0.12491	0.00424	1874	34	1949	28	2028	59
BLS04-08	231	91.7	1088	0.08	0.16650	0.00300	3.47897	0.06521	0.15140	0.00314	993	17	1523	15	2362	35
BLS04-09	53.5	68.4	96.7	0.71	0.38966	0.00815	8.30667	0.23332	0.15445	0.00456	2121	38	2265	25	2396	49
BLS04-10	136	91.5	215	0.42	0.44652	0.00855	11.0036	0.23462	0.17853	0.00410	2380	38	2523	20	2639	38
BLS04-11	372	709	1103	0.64	0.22867	0.00412	4.82624	0.08739	0.15289	0.00306	1328	22	1790	15	2379	34
BLS04-12	127	136	287	0.47	0.33095	0.00625	6.96350	0.14794	0.15242	0.00350	1843	30	2107	19	2373	39
BLS04-13	141	112	288	0.39	0.37358	0.00701	8.03469	0.16147	0.15578	0.00338	2046	33	2235	18	2410	36
BLS04-14	5.22	85.1	254	0.34	0.01686	0.00061	0.11366	0.03647	0.04883	0.01574	108	4	109	33	140	621
BLS04-15	238	87.3	602	0.15	0.34505	0.00629	6.53367	0.11739	0.13715	0.00269	1911	30	2050	16	2192	34

续表 3

Continued Table 3

测点号	含量(×10^-6)			Th/U	同位素比值						年龄(Ma)					
	Pb*	Th	U		$^{206}Pb/^{238}U$	2σ	$^{207}Pb/^{235}U$	2σ	$^{207}Pb/^{206}Pb$	2σ	$^{206}Pb/^{238}U$	2σ	$^{207}Pb/^{235}U$	2σ	$^{207}Pb/^{206}Pb$	2σ
BLS04-16	20.3	45.0	42.9	1.05	0.32985	0.01001	5.69494	0.40571	0.12506	0.00906	1838	49	1931	62	2030	123
BLS04-18	21.3	50.3	46.3	1.09	0.31079	0.00685	5.26391	0.20125	0.12269	0.00484	1745	34	1863	33	1996	68
BLS04-19	26.5	61.7	56.9	1.09	0.30787	0.00710	5.16508	0.21493	0.12154	0.00520	1730	35	1847	35	1979	74
BLS04-20	2.62	67.5	100	0.67	0.01787	0.00122	0.12274	0.09239	0.04975	0.03759	114	8	118	84	183	1185
BLS04-21	156	123	266	0.46	0.44328	0.00832	9.58911	0.18156	0.15674	0.00318	2365	37	2396	17	2421	34
BLS04-22	192	213	662	0.32	0.20322	0.00397	3.52338	0.08295	0.12564	0.00314	1193	21	1533	19	2038	44
BLS04-23	23.4	51.6	49.7	1.04	0.31423	0.00820	5.35717	0.27105	0.12356	0.00640	1762	40	1878	43	2008	89
BLS04-24	4.13	63.9	200	0.32	0.01667	0.00065	0.11406	0.05187	0.04960	0.02262	107	4	110	47	176	816
BLS04-25	181	1180	1944	0.61	0.07184	0.00150	0.55285	0.02443	0.05581	0.00254	447	9	447	16	444	98
BLS04-26	392	109	953	0.11	0.35203	0.00653	6.18103	0.10827	0.12735	0.00238	1944	31	2002	15	2062	33
BLS04-27	20.6	53.1	44.3	1.20	0.29385	0.00723	5.56902	0.24246	0.13748	0.00616	1661	36	1911	37	2196	76
BLS04-28	22.4	62.6	50.4	1.24	0.29365	0.00974	4.90882	0.35472	0.12129	0.00895	1660	49	1804	61	1975	126
BLS04-29	11.3	192	556	0.35	0.01666	0.00041	0.11102	0.01274	0.04838	0.00561	107	3	107	12	118	253
BLS04-30	4.62	174	156	1.11	0.01790	0.00065	0.19840	0.02838	0.08047	0.01177	114	4	184	24	1209	264

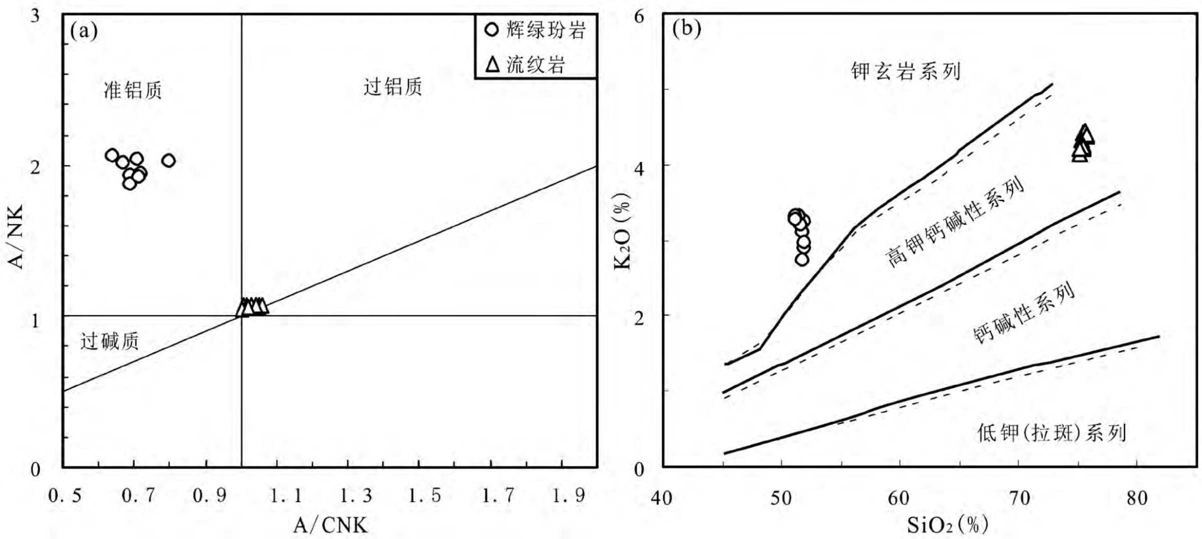

图 5 灵山岛流纹岩和辉绿玢岩 A/CNK-A/NK 图解(a,据 Maniar and Piccoli, 1989)和 SiO_2-K_2O 图解(b,据 Peccerillo and Taylor, 1976; Middlemost, 1985)

Fig.5 Diagrams of A/CNK vs. A/NK (a, after Maniar and Piccoli, 1989) and SiO_2 vs. K_2O (b, after Peccerillo and Taylor, 1976; Middlemost, 1985) for the rhyolite and diabase porphyrite dyke from Lingshan Island

2 颗锆石核部的 $^{207}Pb/^{206}Pb$ 年龄为 2012Ma 和 2028Ma(图 8a),这与围岩地层中的碎屑锆石的峰值年龄 2.0Ga 和 ~700Ma 相对应,而 ~700Ma 年龄表明该地区有华南的物源供应(Wang *et al.*, 2014),因此,解释为岩浆侵位过程中捕获的围岩地层中的锆石年龄;其余 20 个锆石测点的 $^{206}Pb/^{238}U$ 年龄集中于 110~125Ma,加权平均年龄为 118±2Ma,解释为流纹岩的侵位年龄(表 3;图 8b)。

辉绿玢岩样品(BLS04)中的锆石按照形态可以划分为两类,第一类呈半自形-自形长柱状,长轴粒径介于 80~130μm,长宽比 3∶2~2∶1,CL 图像显示锆石发光性好,可见明显的岩浆振荡环带(图 7b)。锆石的 Th、U 含量分别为 63.9×10^{-6}~297×10^{-6} 和 100×10^{-6}~583.7×10^{-6},Th/U 比值为 0.32~1.11,平均为 0.55(表 3),显示岩浆成因锆石的特点(Hoskin and Black, 2000; Belousova *et al.*, 2002;

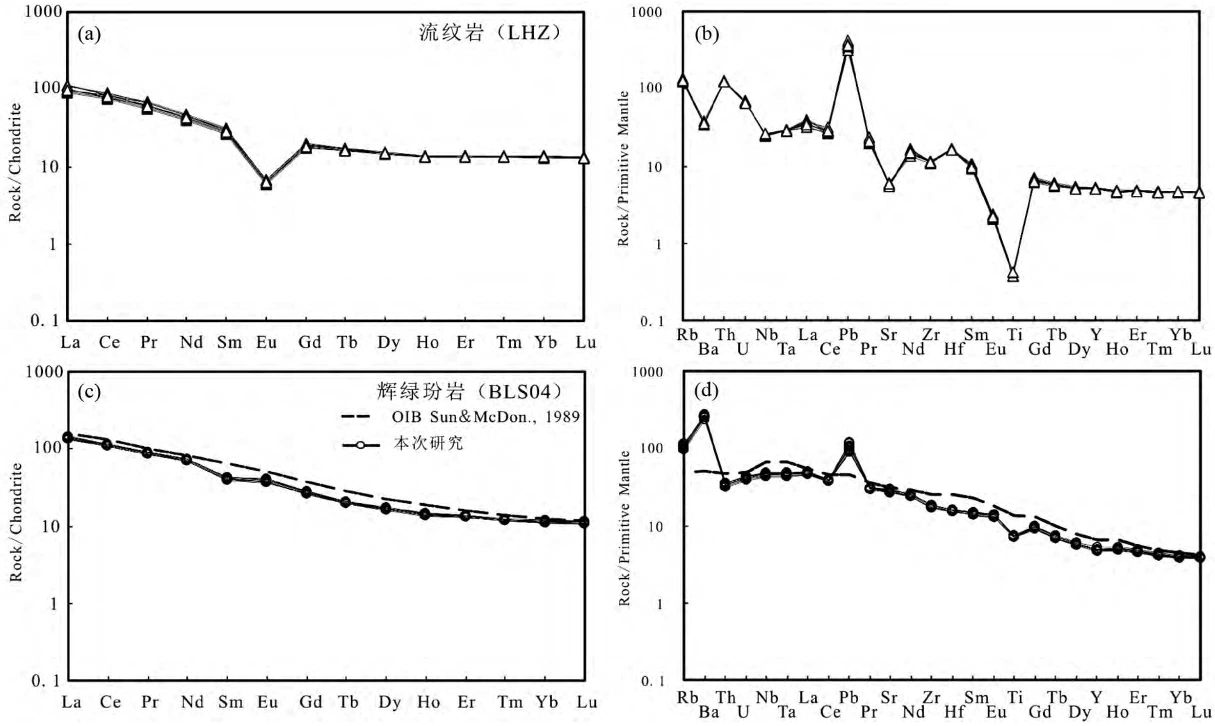

图6 灵山岛流纹岩和辉绿玢岩球粒陨石标准化稀土元素配分曲线和原始地幔标准化微量元素蛛网图(标准化值据 Sun and McDonough,1989)

Fig. 6 Chondrite-normalized REE patterns and primitive mantle-normalized trace element patterns for the rhyolite and diabase porphyrite dyke from the Lingshan Island (normalization values after Sun and McDonough, 1989)

图7 灵山岛流纹岩和辉绿玢岩样品中代表性锆石 CL 图像特征

实线圈为 U-Pb 定年测点位置; 虚线圈为 Lu-Hf 同位素测点位置

Fig. 7 Representative CL images for zircons in the rhyolite and diabase porphyrite from the Lingshan Island

The solid line represents zircon U-Pb dating location; the dotted line represents zircon Lu-Hf measuring location

Hoskin and Schaltegger, 2003)。第二类锆石呈他形椭圆状，长轴粒径介于60~100μm，长宽比为1∶1~3∶2，锆石CL图像显示锆石发光性强，岩浆振荡环带不明显(图7b)，Th/U比值变化较大，集中于0.08~2.03之间(表3)。随机选取样品(BLS04)中30个锆石测点进行原位U-Pb年龄分析，除了剔除的1个年龄外，其余锆石测点结果主体上可分为4组

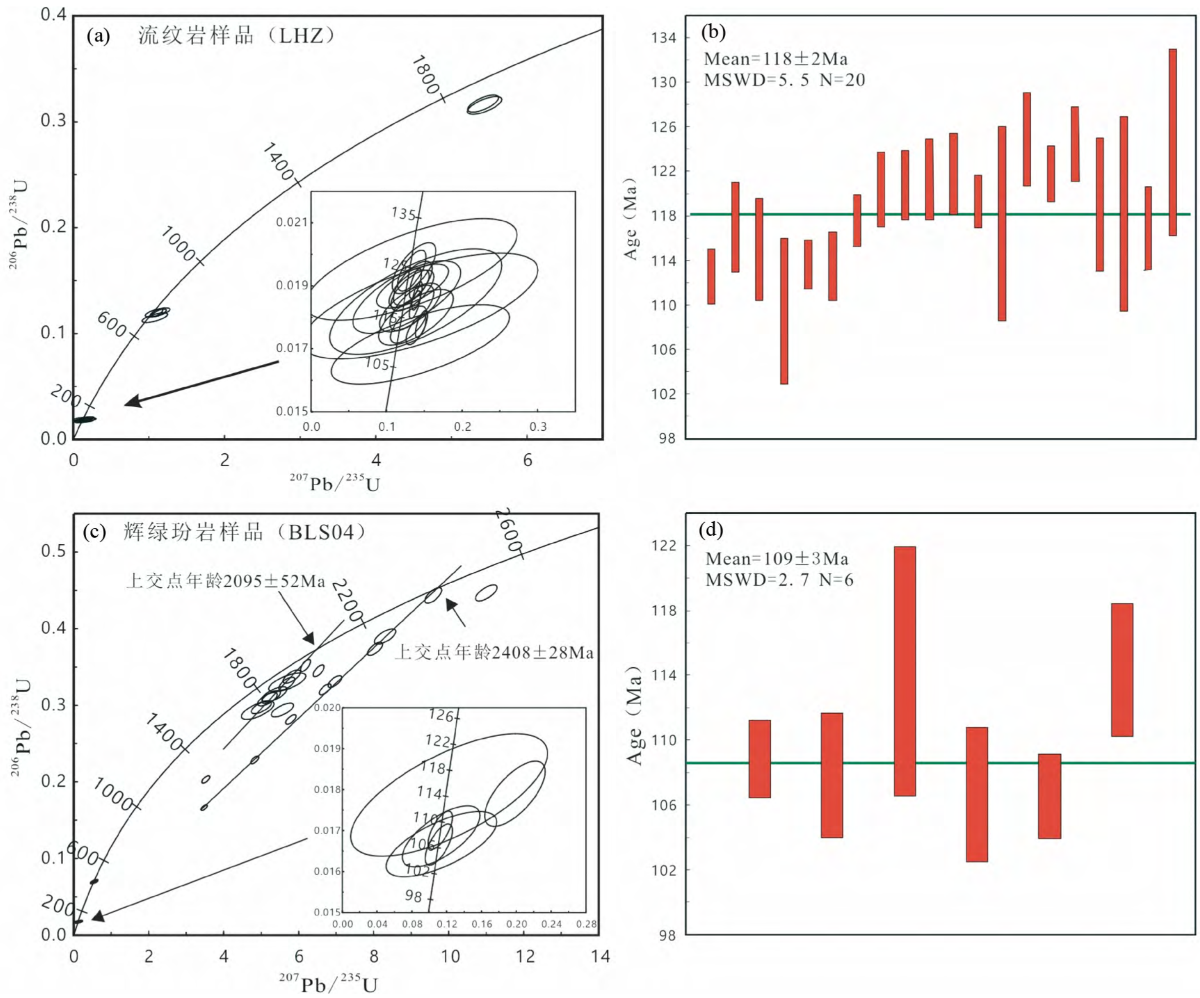

图8 灵山岛流纹岩和辉绿玢岩 LA-ICP-MS 锆石 U-Pb 年龄谐和图和加权平均年龄

Fig. 8 Zircon U-Pb concordia diagrams and weighted mean $^{206}Pb/^{238}U$ ages for the rhyolite and diabase porphyrite dyke from Lingshan Island

(图8c):第一组锆石测点构成一条不一致线,上交点年龄为2408±28Ma;第二组锆石测点构成的不一致线的上交点年龄为2095±52Ma;第三组锆石测点落在谐和线上,2个测点的$^{206}Pb/^{238}U$年龄分别为435±13Ma和447±9Ma;第四组锆石测点的$^{206}Pb/^{238}U$年龄集中于107~114Ma,加权平均年龄为109±3Ma(图8d)。锆石CL图像显示,前三组锆石均呈他形浑圆状,而第四组锆石呈半自形-自形柱状。因此,将447~2408Ma的锆石年龄解释为捕获锆石年龄,而将109±3Ma的年龄解释为辉绿玢岩岩墙侵位时代。这与观察到的辉绿玢岩岩墙侵入到砂岩-含砾砂岩地层中的事实一致。

4.3 锆石 Lu-Hf 同位素组成

锆石Lu-Hf同位素分析是在U-Pb定年的同一部位或结构相同的邻近部位进行的,分析结果见表4。$^{176}Hf/^{177}Hf$初始比值和$\varepsilon_{Hf}(t)$值是根据锆石结晶年龄或者$^{206}Pb/^{238}U$加权平均年龄计算的。

流纹岩样品中,4颗新元古代(702~730Ma)捕获锆石的$^{176}Hf/^{177}Hf$=0.281890~0.282052,计算的$\varepsilon_{Hf}(t)$值为-16.0~-10.3,对应的两阶段模式年龄(t_{DM2})为2249~1981Ma(图9);2颗古元古代(~2.0Ga)捕获锆石的$^{176}Hf/^{177}Hf$=0.281208~0.281238,计算的$\varepsilon_{Hf}(t)$值为-10.8~-10.0,对应两阶段模式年龄(t_{DM2})为3045~3006Ma;其余结晶年龄为118±2Ma的锆石的$^{176}Hf/^{177}Hf$为0.281832~0.282013,计算的$\varepsilon_{Hf}(t)$值介于-31.0~-24.5之间,对应的两阶段模式年龄(t_{DM2})为2535~2212Ma,指示灵山岛流纹岩是由古老陆壳物质部分熔融形成的。

辉绿玢岩样品中,太古代-古元古代锆石颗粒的$^{176}Hf/^{177}Hf$比值介于0.281089~0.281487,计算的$\varepsilon_{Hf}(t)$值为-11.7~2.7,对应的两阶段模式年龄(t_{DM2})为3112~2555Ma;古生代(430~440Ma)锆石的$^{176}Hf/^{177}Hf$比值介于0.282299~0.282434,计算的$\varepsilon_{Hf}(t)$值为-7.8~-2.7,对应的两阶段模式年龄(t_{DM2})为1390~1372Ma。代表辉绿玢岩

表 4 灵山岛流纹岩和辉绿玢岩锆石 Lu-Hf 同位素测定结果

Table 4 Lu-Hf isotopic compositions of zircons for rhyolite and diabase porphyrite from the Lingshan Island

测点号	年龄(Ma)	$^{176}Yb/^{177}Hf$	2σ	$^{176}Lu/^{177}Hf$	2σ	$^{176}Hf/^{177}Hf$	2σ	$\varepsilon_{Hf}(t)$	2σ	t_{DM1}(Ma)	t_{DM2}(Ma)	$f_{Lu/Hf}$
LHZ 流纹岩												
LHZ-01	730	0.042476	0.000262	0.001000	0.000005	0.281960	0.000021	-13.1	1.3	1816	2124	-0.97
LHZ-02	118	0.153662	0.001220	0.003415	0.000026	0.281946	0.000022	-26.9	1.3	1960	2330	-0.90
LHZ-03	118	0.122030	0.002410	0.002686	0.000051	0.281942	0.000019	-27.0	1.2	1926	2335	-0.92
LHZ-04	728	0.085273	0.001380	0.001812	0.000027	0.282052	0.000024	-10.3	1.4	1725	1981	-0.95
LHZ-05	118	0.088974	0.000692	0.002062	0.000015	0.281894	0.000029	-28.6	1.5	1963	2420	-0.94
LHZ-06	118	0.054246	0.000331	0.001301	0.000007	0.281953	0.000028	-26.5	1.4	1841	2312	-0.96
LHZ-07	118	0.286478	0.001330	0.006518	0.000029	0.281977	0.000027	-26.1	1.4	2098	2286	-0.80
LHZ-08	118	0.083475	0.002530	0.001988	0.000056	0.281962	0.000029	-26.2	1.5	1862	2298	-0.94
LHZ-09	2020	0.018836	0.000053	0.000439	0.000001	0.281208	0.000020	-10.8	1.9	2807	3045	-0.99
LHZ-10	2020	0.027761	0.000068	0.000635	0.000001	0.281238	0.000017	-10.0	1.8	2780	3006	-0.98
LHZ-11	118	0.272855	0.001680	0.006088	0.000038	0.281998	0.000022	-25.3	1.3	2036	2246	-0.82
LHZ-12	118	0.204211	0.006700	0.004566	0.000149	0.281930	0.000026	-27.5	1.4	2049	2362	-0.86
LHZ-13	118	0.091786	0.000236	0.002085	0.000006	0.281886	0.000021	-28.9	1.3	1975	2433	-0.94
LHZ-15	118	0.152532	0.001720	0.003494	0.000043	0.281976	0.000022	-25.8	1.3	1920	2278	-0.89
LHZ-17	118	0.144345	0.000324	0.003195	0.000011	0.281940	0.000022	-27.1	1.3	1957	2341	-0.90
LHZ-18	118	0.247202	0.004170	0.005668	0.000099	0.282013	0.000028	-24.7	1.4	1988	2220	-0.83
LHZ-19	118	0.094256	0.002510	0.002309	0.000064	0.281928	0.000026	-27.5	1.4	1927	2360	-0.93
LHZ-20	728	0.051391	0.000382	0.001274	0.000011	0.282027	0.000020	-10.9	1.3	1736	2013	-0.96
LHZ-21	118	0.138491	0.000428	0.003135	0.000009	0.281943	0.000020	-27.0	1.3	1950	2336	-0.91
LHZ-22	118	0.205612	0.000529	0.004588	0.000013	0.281971	0.000022	-26.1	1.3	1989	2291	-0.86
LHZ-23	701	0.029164	0.000488	0.000664	0.000010	0.281890	0.000018	-16.0	1.3	1896	2249	-0.98
LHZ-25	118	0.088780	0.001140	0.002032	0.000024	0.281931	0.000020	-27.3	1.2	1909	2354	-0.94
LHZ-26	118	0.161811	0.002420	0.003946	0.000053	0.281832	0.000036	-31.0	1.6	2161	2535	-0.88
LHZ-27	118	0.091193	0.001390	0.002159	0.000031	0.282011	0.000024	-24.5	1.3	1801	2212	-0.93
LHZ-29	118	0.077499	0.000581	0.001799	0.000012	0.281880	0.000020	-29.1	1.2	1968	2443	-0.95
LHZ-30	118	0.114416	0.001500	0.002631	0.000036	0.281872	0.000025	-29.4	1.3	2024	2459	-0.92
BLS04 辉绿玢岩												
BLS04-01	108	0.105671	0.001740	0.002457	0.000037	0.281829	0.000019	-31.2	1.2	2077	2538	-0.93
BLS04-02	436	0.099111	0.002100	0.002252	0.000047	0.282299	0.000023	-7.8	1.4	1390	1620	-0.93
BLS04-03	2408	0.030448	0.000204	0.000659	0.000005	0.281089	0.000010	-6.6	1.3	2982	3152	-0.98
BLS04-04	2408	0.024149	0.000446	0.000565	0.000011	0.281215	0.000008	-2.0	1.3	2806	2925	-0.98
BLS04-05	2095	0.044384	0.000042	0.000951	0.000002	0.281479	0.000011	-0.2	1.6	2475	2583	-0.97
BLS04-06	2095	0.024220	0.000388	0.000519	0.000008	0.281255	0.000014	-7.6	1.7	2749	2946	-0.98
BLS04-07	2095	0.029912	0.000096	0.000620	0.000002	0.281328	0.000011	-5.1	1.6	2658	2825	-0.98
BLS04-08	2408	0.038402	0.000215	0.000873	0.000005	0.281156	0.000010	-4.6	1.3	2908	3052	-0.97
BLS04-09	2408	0.022522	0.000049	0.000506	0.000002	0.281346	0.000012	+2.7	1.3	2626	2692	-0.98
BLS04-10	2640	0.035215	0.000069	0.000763	0.000001	0.281106	0.000011	-1.0	1.4	2968	3064	-0.98
BLS04-11	2408	0.073942	0.000334	0.001582	0.000007	0.281155	0.000012	-5.8	1.3	2965	3112	-0.95
BLS04-12	2408	0.015350	0.000116	0.000348	0.000003	0.281176	0.000010	-3.0	1.3	2843	2976	-0.99
BLS04-13	2408	0.038908	0.000048	0.000816	0.000001	0.281138	0.000010	-5.1	1.3	2928	3079	-0.98
BLS04-14	108	0.099356	0.000364	0.002483	0.000014	0.281837	0.000016	-30.9	1.2	2067	2524	-0.93
BLS04-15	2191	0.011717	0.000129	0.000290	0.000003	0.281336	0.000009	-2.2	1.4	2625	2759	-0.99
BLS04-16	2095	0.037403	0.000121	0.000800	0.000003	0.281465	0.000009	-0.5	1.6	2485	2598	-0.98
BLS04-18	2095	0.034448	0.000339	0.000768	0.000009	0.281433	0.000012	-1.6	1.7	2525	2651	-0.98
BLS04-19	2095	0.027840	0.000090	0.000691	0.000003	0.281463	0.000012	-0.4	1.7	2479	2593	-0.98
BLS04-20	108	0.055539	0.000334	0.001333	0.000007	0.282910	0.000015	+7.1	1.2	490	594	-0.96
BLS04-21	2408	0.042640	0.000243	0.001005	0.000006	0.281279	0.000009	-0.5	1.3	2751	2849	-0.97
BLS04-22	2037	0.038598	0.000325	0.000854	0.000008	0.281188	0.000010	-11.7	1.5	2864	3103	-0.97
BLS04-23	2095	0.035977	0.000048	0.000762	0.000000	0.281487	0.000009	+0.3	1.6	2451	2555	-0.98
BLS04-24	108	0.064612	0.000549	0.001554	0.000012	0.281837	0.000011	-30.8	1.1	2016	2522	-0.95
BLS04-25	447	0.084288	0.000527	0.002030	0.000020	0.282434	0.000020	-2.7	1.3	1188	1372	-0.94
BLS04-26	2095	0.002681	0.000031	0.000057	0.000001	0.281315	0.000009	-4.8	1.6	2637	2808	-1.00
BLS04-27	2196	0.052186	0.000197	0.001122	0.000004	0.281465	0.000015	+1.3	2.1	2505	2591	-0.97
BLS04-28	2095	0.066723	0.000281	0.001430	0.000004	0.281476	0.000025	-1.0	1.8	2510	2622	-0.96
BLS04-29	108	0.120506	0.000369	0.002866	0.000009	0.281895	0.000014	-28.8	1.1	2004	2421	-0.91
BLS04-30	108	0.108216	0.000159	0.002555	0.000008	0.282940	0.000017	+8.1	1.2	461	542	-0.92

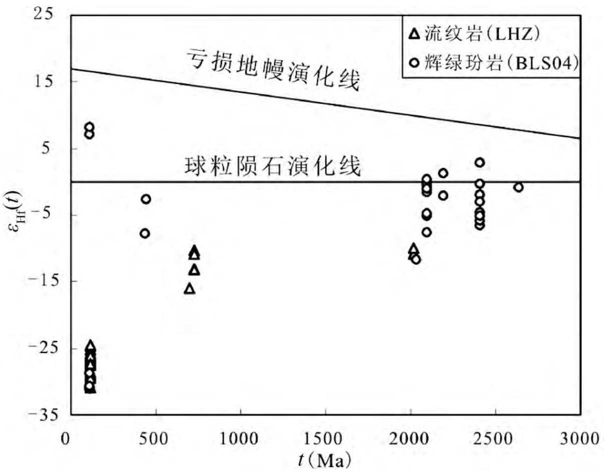

图9 灵山岛流纹岩和辉绿玢岩锆石 Hf 同位素组成(球粒陨石演化线和亏损地幔演化线据 Blichert-Toft and Albarède, 1997; Griffin *et al.*, 2002)

Fig. 9 Zircon Hf isotope compositions for rhyolite and diabase porphyrite dyke from the Lingshan Island (the evolutionary trends of chondrite and depleted mantle are from Blichert-Toft and Albarède, 1997; Griffin *et al.*, 2002)

结晶年龄(109±3Ma)的6颗锆石的 Hf 同位素组成不均一,其中,2个锆石测点(点20和30)的$^{176}Hf/^{177}Hf$比值较高,为0.282910和0.282940,计算的$\varepsilon_{Hf}(t)$值分别为+7.1和+8.1,对应的单阶段模式年龄(t_{DM1})分别为490Ma和461Ma;其余4颗锆石的$^{176}Hf/^{177}Hf$比值较低,介于0.281829~0.281895,计算的$\varepsilon_{Hf}(t)$值为-31.2~-28.8,对应的单阶段模式年龄(t_{DM1})为2077~2004Ma,两阶段模式年龄(t_{DM2})为2538~2421Ma。一般来讲,锆石具有很高的 Hf 同位素体系封闭温度,甚至在麻粒岩等高级变质作用下,仍可保持原始的 Hf 同位素组成(吴福元等,2007b)。也就是说,锆石 Hf 同位素可以很好的反映出源区特征。上述基性岩样品中年龄为109±3Ma的锆石同时包含了$^{176}Hf/^{177}Hf$比值较低的4颗锆石和$^{176}Hf/^{177}Hf$比值较高的2颗锆石,很可能是不同来源的岩浆混合作用形成的。

5 讨论

5.1 灵山岛岩浆活动时代

根据前人划分方案,灵山岛这套地层早期通常被认为可与胶莱盆地下白垩统莱阳群法家莹组对比(K_1f),其上部火山-碎屑岩地层被划分为下白垩统青山群八亩地组(K_1b)(山东省第四地质矿产勘查院,2003; 栾光忠等,2010)。灵山岛的岩浆活动可对应早白垩世晚期青山期的岩浆活动。已有研究显示,灵山岛碎屑沉积地层中的碎屑锆石年龄具有2.5~2.3Ga、2.1~1.9Ga、850~700Ma、138~121Ma几个峰值,因此,这套地层的沉积年龄上限(最大沉积时代)被限定为138~121Ma(Wang *et al.*, 2014)。此外,部分学者对作为灵山岛标志层的白色流纹岩进行了锆石 U-Pb 年龄测定,获得了119.2Ma和123.9Ma的成岩年龄(Wang *et al.*, 2014; 周瑶琪等,2015b)。本文选取灵山岛南部流纹岩和灵山岛北部辉绿玢岩样品进行了锆石原位 U-Pb 年龄测定。流纹岩中获得两组捕获锆石年龄分别为702~730Ma和~2.0Ga,流纹岩的形成年龄为118±2Ma。可以看出,流纹岩中捕获锆石年龄与 Wang *et al.* (2014)获得的部分碎屑锆石年龄基本一致。辉绿玢岩样品中的锆石年龄复杂,获得了2408±28Ma、2095±52Ma、~440Ma和109±3Ma四组年龄。对比锆石 CL 图像特征发现,形成年龄为109±3Ma的锆石呈细小半自形-自形柱状,而其它锆石大部分呈浑圆状,无环带结构。据此,辉绿玢岩的形成时代可以被限定在109±3Ma。野外地质特征显示该岩墙切穿碎屑岩层,因此,结合碎屑锆石年龄(Wang *et al.*, 2014),灵山岛地层沉积时代可被限定在121~109Ma之间。

综上所述,同华北东部大部分地区一样(Zhou and Li, 2000; 翟明国和樊祺诚等,2002; 翟明国等,2004; Wu *et al.*, 2005; Yang *et al.*, 2008; 朱日祥等,2011; Zhai and Santosh, 2013; Liu *et al.*, 2015; 刘燊等,2016; Li *et al.*, 2018),灵山岛广泛发育的中生代岩浆活动时代为早白垩世(124~105Ma),岩石类型以酸性火山岩和基性岩墙为代表,基性岩墙的形成时代略晚于酸性火山岩。

5.2 岩石成因和岩浆源区

主量元素显示,流纹岩样品具有高的SiO_2、K_2O/Na_2O比值和全碱含量($K_2O+Na_2O=8.83\%\sim9.06\%$),以及低的CaO、MgO含量的特征,与A型花岗岩类似。但是,该流纹岩样品具有相对偏低的Ga/Al比值($10^4\times Ga/Al=2.60\sim2.66$)、Rb/Sr比值(0.65~0.75)以及$Fe_2O_3^T/MgO$比值,较低的Zr、Nb、Ce、Y含量($Zr+Nb+Ce+Y=206\times10^{-6}\sim223\times10^{-6}$)、$TiO_2$含量以及较低的锆石结晶温度(761~771℃)(Watson and Harrison, 1983),这些特征又不同于典型的A型花岗岩(Collins *et al.*, 1982; Whalen *et al.*, 1987; 吴福元等,2007a)。岩石样品高硅富碱,低CaO、Fe-Mg、TiO_2、P_2O_5的特征表明岩浆经历了一定程度的分异演化。其相对富铝,具Eu负异常,Ba、Sr相对亏损,Rb、U相对富集,以及较低的Zr含量、Zr/Hf(24.6~25.5)、Nb/Ta(14.5~15.7)比值等特征显示出与高分异的I型花岗岩一致的特征。在花岗岩岩石成因类型判别图解中(图10b)(Sylvester, 1989),所有流纹岩样品落入高分异钙碱性花岗岩范围内;在$Fe_2O_3^T/MgO$-(10000×Ga/Al)和(K_2O+Na_2O)/CaO-(Zr+Nb+Ce+Y)的判别图解中(图11),分析样品分别落入分异的I长英质花岗岩和分异的长英质花岗岩-A型花岗岩区域,支持上述结论。尽管要区分高分异的I型和S型花岗岩难度较大(Chappell, 1999; 吴福元等,2007a, 2017; Gao *et al.*, 2016),但是鉴于上述地球化学特征及该流纹岩弱过铝质的

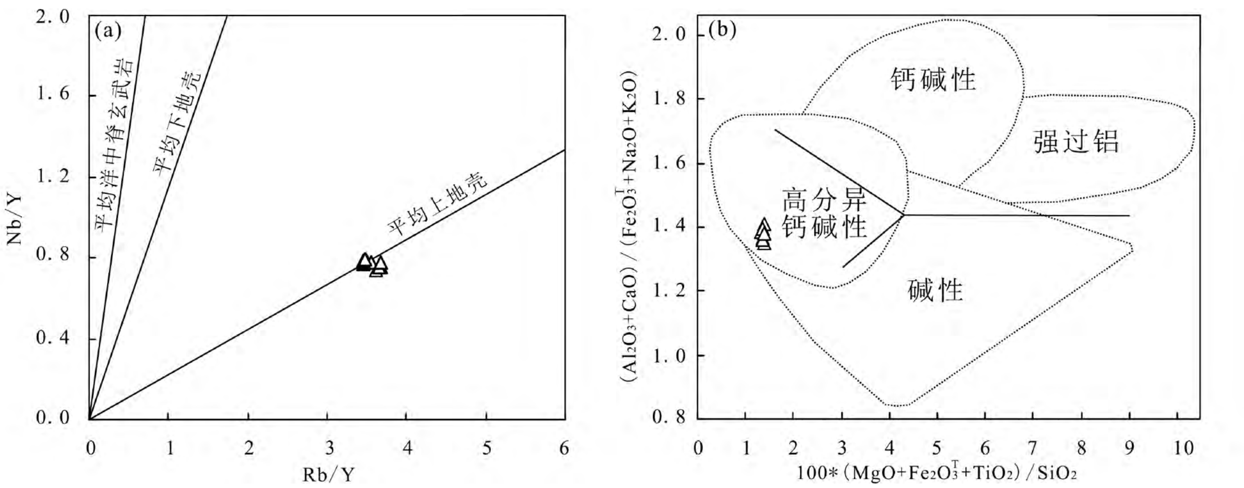

图 10 灵山岛流纹岩 Rb/Y-Nb/Y 判别图解(a,据 Hildreth *et al.*,1991)和花岗岩岩石成因类型判别图(b,据 Sylvester,1989)

Fig. 10 Rb/Y vs. Nb/Y discrimination diagram (a, after Hildreth *et al.*, 1991) and chemical discrimination diagram (b, after Sylvester, 1989) of the rhyolite from Lingshan Island

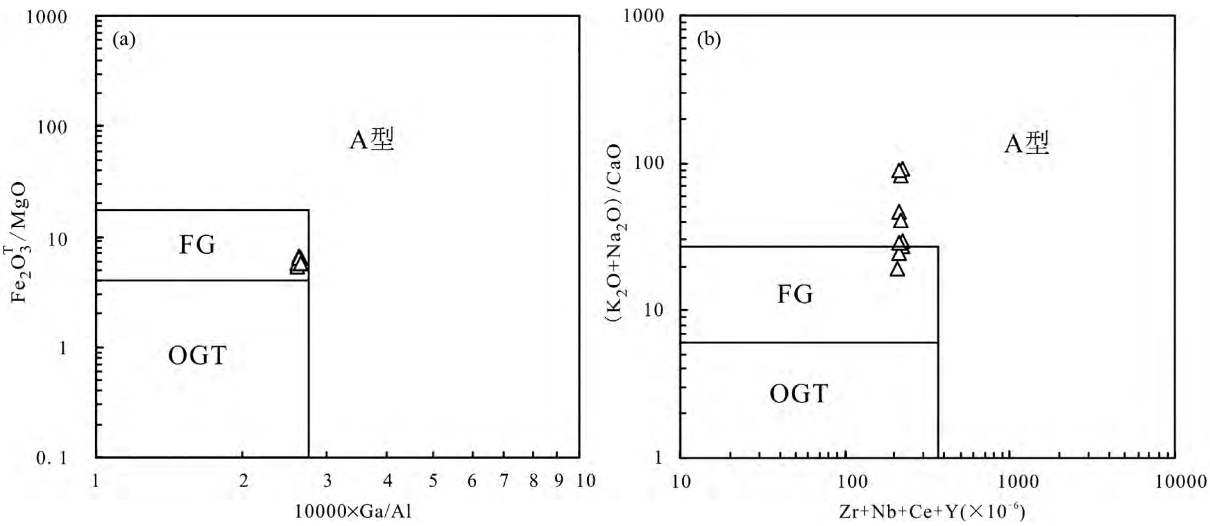

图 11 灵山岛流纹岩地球化学分类图解(据 Whalen *et al.*,1987)

FG: 分异的长英质花岗岩; OGT: 未分异的 M、I、S 花岗岩

Fig. 11 The geochemical classifacation diagrams for the rhyolite from Lingshan Island (after Whalen *et al.*, 1987)

FG: Fractionated felsic granites; OGT: unfractionated M-, I-and S-type granites

特征(A/CNK = 1.00 ~ 1.06)、低 P_2O_5 含量(0.01% ~ 0.07%)以及较高的 Na_2O 含量(4.58% ~4.87%)的特征,本文认为灵山岛流纹岩样品与高分异的 I 型花岗岩地球化学特征类似。

流纹岩样品轻、重稀土元素分异较弱($(La/Yb)_N$ = 6.42 ~8.09),重稀土平坦,指示岩浆源区部分熔融残留相主要矿物组成是角闪石而非石榴石;Eu、Sr、Ba 负异常指示斜长石在岩浆源区是稳定的,或者岩浆演化过程中有斜长石的结晶分异(Xiong *et al.*,2005);无明显的 Nb-Ta 负异常,指示源区部分熔融残留相中无金红石;此外,样品的 Sr 含量相对较低($114\times10^{-6} \sim 125\times10^{-6}$)而 Yb 含量相对较高($2.21\times10^{-6} \sim 2.30\times10^{-6}$),这些特征均表明灵山岛流纹岩可能是壳源物质在压力较小条件下(地壳浅部)部分熔融形成的。流纹岩的成因及物质来源复杂,主要有三种认识:①地壳物质受幔源岩浆底侵发生部分熔融形成(王德滋等,1994; 于津海等,1998; 李伍平,2011);②幔源玄武质岩浆经分离结晶作用形成(Whalen *et al.*,1987; McCulloch *et al.*,1994; Shinjo and Kato,2000; Wu *et al.*,2002; 陈志洪等,2013);③壳幔

岩浆混合形成(Hildreth *et al.*，1991; Turner *et al.*，1992; 李献华等，2002; Briand *et al.*，2002; Yang *et al.*，2006; 丁烁等，2011)。通常情况下，流纹岩并不能由幔源岩浆直接分异形成，幔源玄武质岩浆结晶分异一般形成的是安山质岩石(Hirose，1997)。该流纹岩样品具有低的 $Mg^{\#}$ 值(26.1～30.4)和低的 Cr($0.89\times10^{-6}\sim5.95\times10^{-6}$)、Ni($1.09\times10^{-6}\sim4.42\times10^{-6}$)含量，以及高 Si、高 Rb、Th、Pb 含量(图 6b)和低 Sm/Nd 比值(0.21～0.22)，且在野外并未发现壳幔岩浆混合的证据，排除地幔物质的加入。Rb/Y-Nb/Y 图解可以判断岩石物质来源或受混染的程度，因为 Rb/Nb 比值有规律地从地幔向上地壳增大，平均洋中脊玄武岩(N-MORB) Rb/Nb 比值为 0.36，平均下地壳比值为 0.88，平均上地壳比值为 4.5。而 Y 在各类岩石中丰度较高、变化范围较小(Hildreth *et al.*，1991)。因此，在 Rb/Y-Nb/Y 图解中(图 10a)，所有样品落在平均上地壳演化线上及其附近，表明其源于上地壳。流纹岩中的锆石具有极负的 $\varepsilon_{Hf}(t)$ 值(−31.0～−24.5)，两阶段模式年龄为 2535～2212Ma，远远老于锆石结晶年龄，亦指示岩浆源区为古老地壳物质，无地幔物质加入。因此，灵山岛流纹岩可能是软流圈地幔物质上涌、底侵，导致上覆古老地壳物质在浅部伸展环境下部分熔融形成后，产生的岩浆经历了一定程度结晶分异演化而形成。

对于灵山岛辉绿玢岩而言，本文所获得的样品具有较高的烧失量，指示其可能受到后期蚀变作用的影响，因此，K、Na 等活动性元素不能用来判别岩石成因和构造环境等。已有研究表明，高场强元素 Nb、Ta、Zr、Hf 和相容元素 Cr、Co、Ni，以及稀土元素在变质作用过程中属于不活动元素，可以用来判别岩石成因及其形成环境(Kerrich *et al.*，1999; Hastie *et al.*，2007)。通常情况下，玄武质岩浆受地壳物质同化混染会表现出明显的 Nb、Ta 负异常和 Zr、Hf 正异常(Sun and McDonough，1989; Zhao and Zhou，2007)。而且，大洋玄武岩的 Nb/U 平均比值为 37～67(Hofmann *et al.*，1986; Hofmann，2003)，明显高于地壳的比值 6.2(Rudnick and Gao，2003)，Nb/U 比值可以反映玄武质岩浆受地壳物质同化混染的情况。微量元素原始地幔标准化蛛网图显示，灵山岛辉绿玢岩无 Nb、Ta、Zr 和 Hf 的异常(图 6d)，其 Nb/U 比值较高(36～38)。指示该样品形成过程中未受到或受到轻微地壳物质混染。此外，辉绿玢岩样品低的 Th/Nb 比值(0.09)、La/Nb(0.97～1.04)比值和高的 Nb/Zr 比值(0.16～0.17)、Nb/Ta 比值(17.1～17.5)也支持其形成过程中未受到明显地壳物质混染的特征。尽管辉绿玢岩中包含大量年龄较老的锆石，但是本文认为老的锆石为岩墙侵位晚期捕获浅部围岩地层中的锆石，与岩浆房中地壳物质混染无关。首先，辉绿玢岩无明显地壳混染的地球化学特征。如果老的锆石在深部岩浆房中捕获，这一过程需要同化大量的地壳物质和较长的滞留时间，这必然会导致玄武质岩浆化学成分的改变。其次，捕获的锆石年龄分布广泛(～2400Ma、～2100Ma、～440Ma)，与辉绿玢岩侵入碎屑岩地层并尖灭的野外观察一致。因此，推测玄武质岩浆形成后快速上升并侵入到地壳浅部碎屑岩地层中，捕获了来自碎屑岩地层中的不同时代的锆石，而此时的热力学条件尚不足以使岩浆与围岩发生反应从而产生成分上的改变。

样品的 $Mg^{\#}$ 值(67.6～69.4)、Cr($370\times10^{-6}\sim578\times10^{-6}$)和 Ni($167\times10^{-6}\sim252\times10^{-6}$)元素含量均略低于或接近起源于亏损地幔源区的原始玄武质岩浆成分(Wilkinson，1982; Hofmann，1988)，但岩浆上侵过程中又无明显地壳物质混染，指示岩浆经历了一定程度的分异演化。Cr、Ni 和 MgO 元素协变图解中呈正相关，表明岩浆发生橄榄石或者单斜辉石分离结晶(图 12e，f)。Cr、Ni 协变图解中呈正相关，以及 CaO、MgO 的正相关同样表明发生了单斜辉石分离结晶(图 12a，h)。Al_2O_3 和 MgO 呈负相关以及微弱的 Eu 正异常指示无斜长石分离结晶或少量斜长石的堆晶作用(图 12b、图 6c)。此外，随着 MgO 含量增加，TiO_2、V 元素含量变化不大，而 $Fe_2O_3^T$ 呈增加趋势，表明未发生明显 Fe-Ti 矿物的分离结晶(图 12d，e，g)。

灵山岛辉绿玢岩样品的 Zr/Y 比值为 8.55～9.11，Ti/V 比值为 50.5～54.4，与板内玄武岩特征一致(Pearce and Cann，1973)。在 Nb×2-Zr/4-Y(图 13a; Meschede，1986)、Ti-V(图 13b; Shervais，1982)、Zr-Ti/100-Y×3(图 13c; Pearce and Cann，1973)和 Zr-Zr/Y(图 13d; Pearce and Norry，1979)构造环境判别图解中，所有辉绿玢岩样品均落入板内碱性玄武质岩石区域。此外，Zr、Nb 和 Yb 等非活动性元素可以用来限定地幔源区特征，如 Nb/Yb 比值(Pearce and Stern，2006)。灵山岛辉绿玢岩样品的 Nb/Yb 比值为 16.4～17.4，接近于球粒陨石，而远高于 N-MORB(0.76)和 E-MORB(3.5)的比值(Sun and McDonough，1989)，指示其源于高度富集的地幔源区。一般情况下，Th 易受俯冲带流体影响而富集，但 Nb 可以保持不变。因此，在 Nb/Yb-Th/Yb 图解中(图 14)，样品显示为板内富集，未受到俯冲带流体改造且源区成分介于 E-MORB 和 OIB 之间并接近 OIB 特征，表明岩浆源于板内环境而非岛弧环境。这与多数学者认为华北东部中生代岩浆活动中无明显的古太平洋俯冲板片物质成分的贡献的观点一致(Fan *et al.*，2001; Guo *et al.*，2001; Xu，2001; Qiu *et al.*，2002a，b; Zhang *et al.*，2005)。在部分熔融过程中 Sm/Yb 比值不会变化，但 La/Sm 比值会随部分熔融程度增加而降低(Aldanmaz *et al.*，2000)。在 La/Yb-Dy/Yb 图解中(图 15a)，样品落入尖晶石橄榄岩地幔源区，源区经历了低程度(2%～2.5%)的部分熔融；另外，在 La/Sm-Sm/Yb 判别图解中(图 15b)，样品落于石榴子石+尖晶石二辉橄榄岩地幔源区，发生了低程度(1%～5%)的部分熔融，综上所述，灵山岛辉绿玢岩样品源于中-深部的地幔源区，可能形成于尖晶石和石榴子石稳定相的过渡区域。

前人通过玄武岩和地幔捕掳体的微量元素及 Sr-Nd-Pb 同位素等分析方法，对中国东部中生代的岩石圈(软流圈)地幔性质做了大量研究(Peng *et al.*，1986; Basu *et al.*，1991;

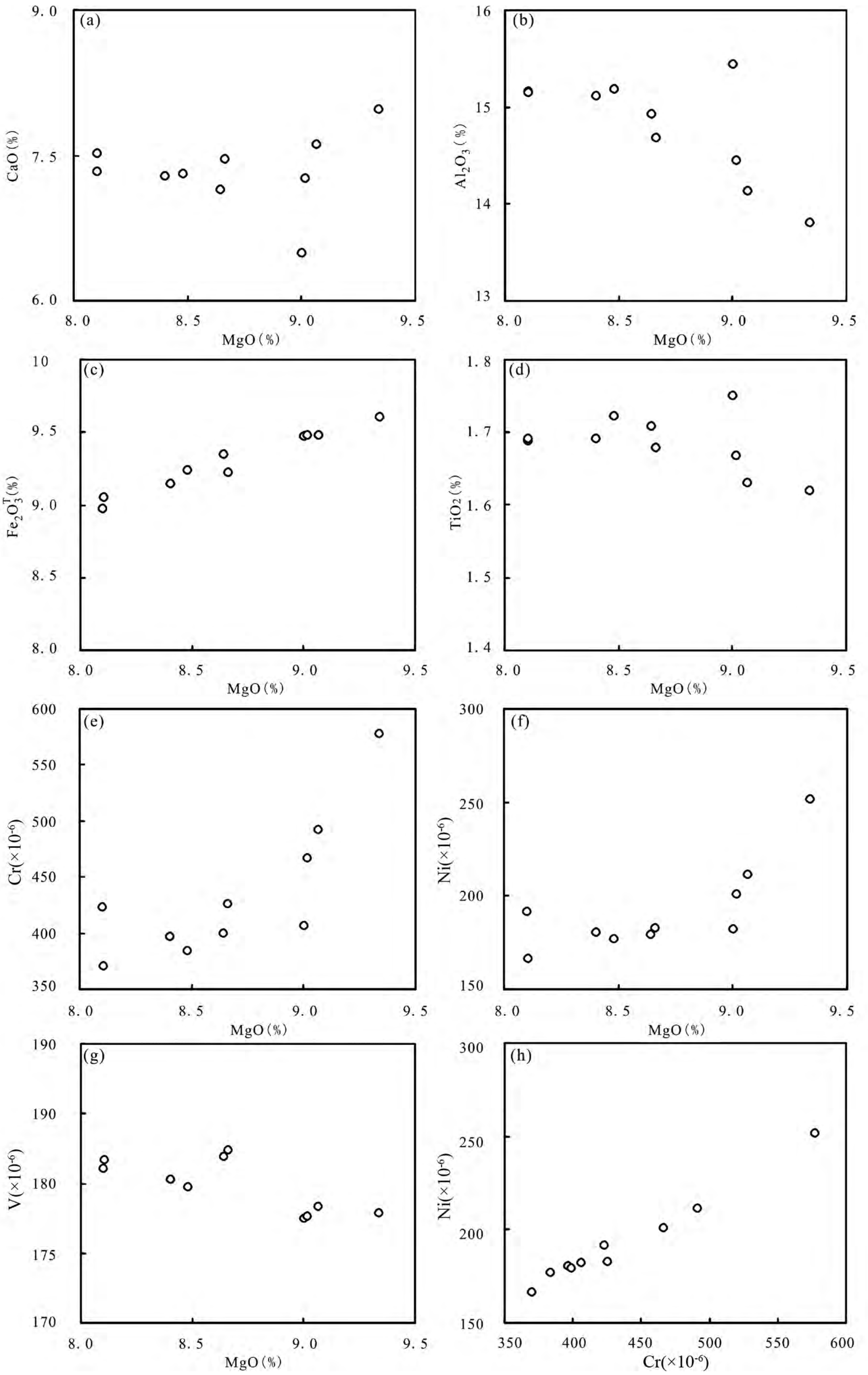

图 12 灵山岛辉绿玢岩主量、微量元素协变图解

Fig. 12 Plots of representative major and trace elements for the diabase porphyrite dyke from Lingshan Island

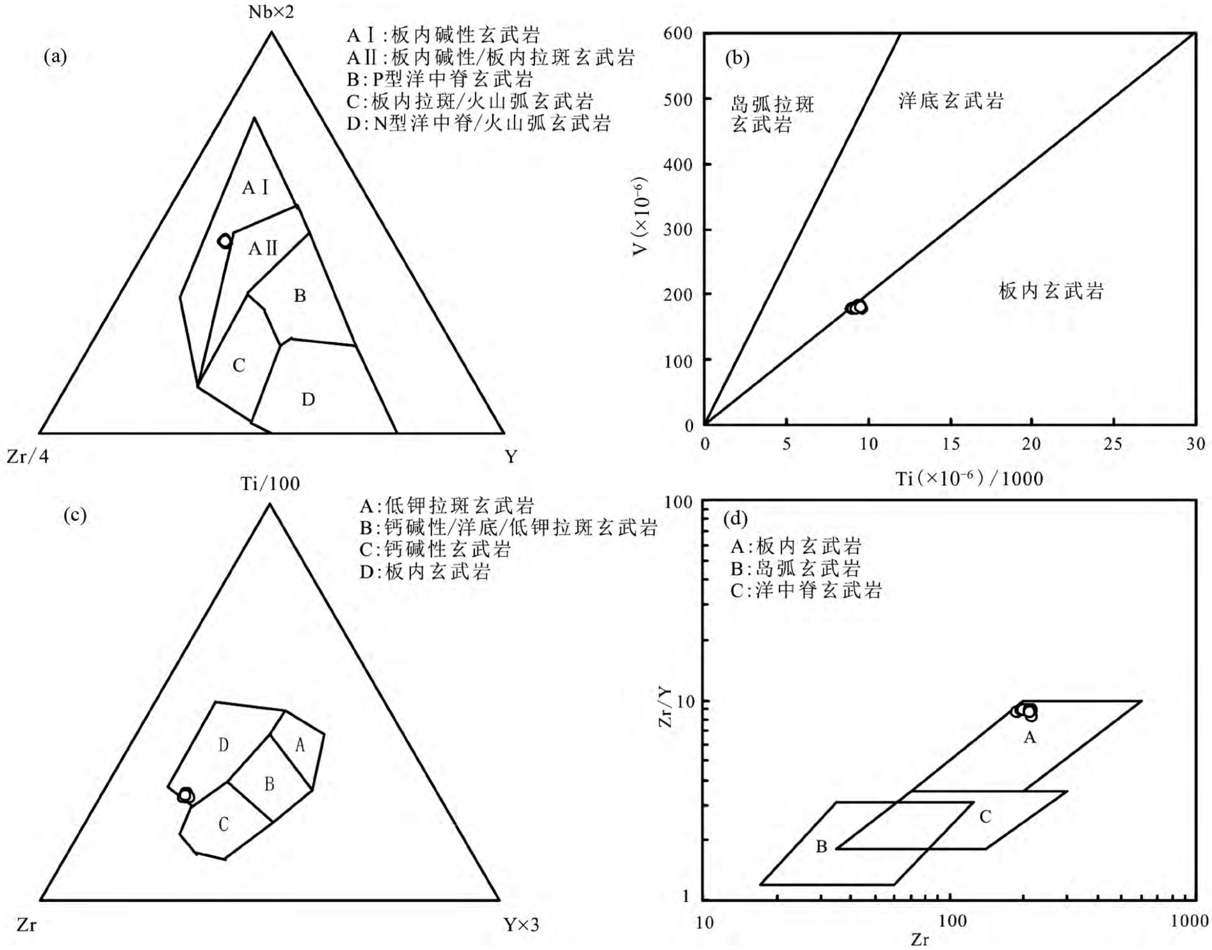

图13 灵山岛辉绿玢岩构造环境判别图解

(a) Nb-Zr-Y 图解(Meschede, 1986); (b) Ti-V 图解(Shervais, 1982); (c) Ti-Zr-Y 图解(Pearce and Cann, 1973); (d) Zr-Zr/Y 图解(Pearce and Norry, 1979)

Fig. 13 Trace element discrimination diagrams for the diabase porphyrite dyke from Lingshan Island

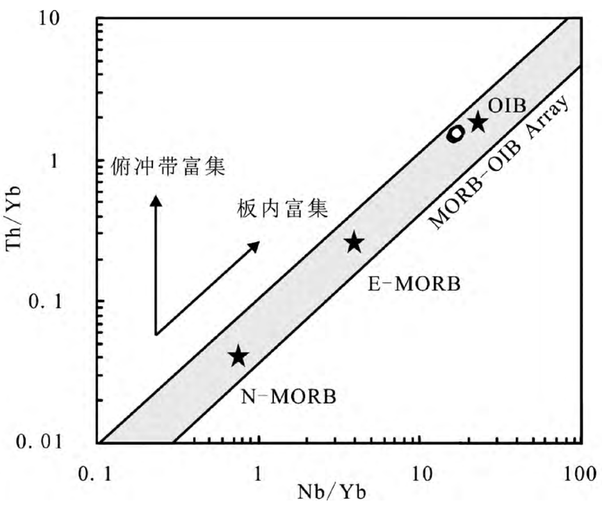

图14 灵山岛辉绿玢岩源区 Nb/Yb-Th/Yb 判别图解(据 Pearce, 2008)

Fig. 14 Nb/Yb vs. Th/Yb discrimination diagramfor the diabase porphyrite dyke from Lingshan Island (after Pearce, 2008)

Fan and Hooper, 1991; Liu *et al.*, 1994; Yan *et al.*, 2008)。结果暗示该时期亏损的软流圈地幔和不同程度富集的岩石圈地幔均参与了玄武岩岩浆的形成。换言之,古老的富集岩石圈地幔与新生的亏损岩石圈地幔共存。导致上述结果的原因可能是是古太平洋-伊泽奈崎(库拉)板块间的洋中脊向亚欧大陆的俯冲或者板块俯冲诱发的大陆深部软流圈地幔上涌(Uyeda and Miyashiro, 1974; Basu *et al.*, 1991)。前已述及,灵山岛辉绿玢岩中的岩浆锆石具有负的 $\varepsilon_{Hf}(t)$ 值(−31.2 ~ −28.8)和正的 $\varepsilon_{Hf}(t)$ 值(+7.1 ~ +8.1),具有相对明显的环带结构,对应的 Th/U 比值较高,指示其为岩浆锆石。因此,正负两种 $\varepsilon_{Hf}(t)$ 值的锆石均为源区岩浆结晶形成(非捕获锆石)。正负两种 $\varepsilon_{Hf}(t)$ 值的锆石并存,然而 Nb/Yb 比值等地球化学特征显示其源区是富集的。表明不同源区的岩浆"混合"作用。因此,该辉绿玢岩可能是起源于有深部亏损软流圈地幔物质加入的富集地幔源区,这与华北东部早白垩世青山群火山岩源区为有软流圈地幔物质加入的富集岩石圈地幔的结论对应(邱检生等, 2001, 2004, 2012; 刘燊等, 2003; 凌文黎等, 2006; 刘勇胜和高山, 2007; Ling *et*

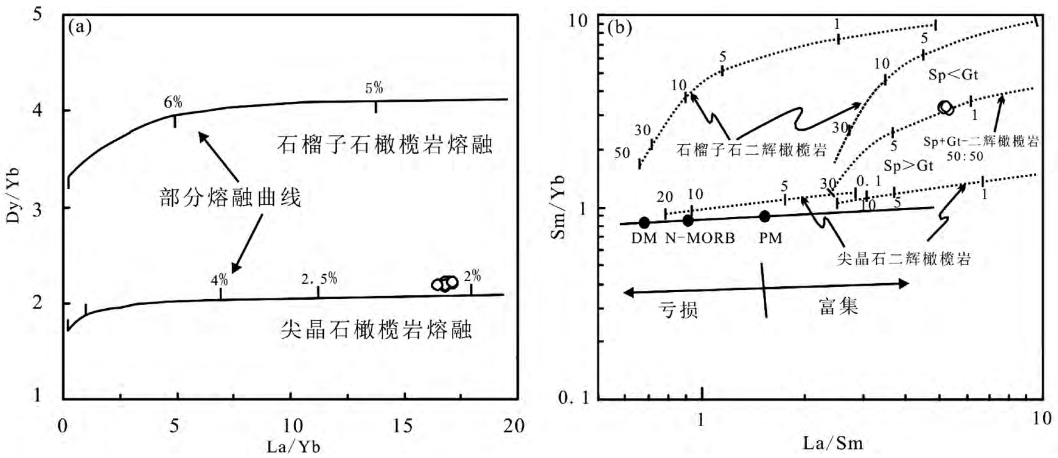

图15 灵山岛辉绿玢岩源区 La/Yb-Dy/Yb 判别图解(a,据 Jung *et al.*, 2006)和 La/Sm-Sm/Yb 判别图解(b,据 Aldanmaz *et al.*, 2000)

Fig. 15 Discrimination diagrams of La/Yb vs. Dy/Yb (a, after Jung *et al.*, 2006) and La/Sm vs. Sm/Yb (b, after Aldanmaz *et al.*, 2000) for the diabase porphyrite dyke from Lingshan Island

al., 2009)。值得注意得是,该时期年轻亏损地幔成分的加入标志华北富集的古老岩石圈地幔的转变,即从克拉通大陆岩石圈地幔变为中生代富集岩石圈地幔,随后再变为新时代亏损型大洋型地幔(吴福元和孙德有,1999; 吴福元等,2008; Xu,2001; Zhang *et al.*, 2003; 周新华,2009),指示区域大地构造进一步向伸展环境发展。

综上所述,灵山岛流纹岩和辉绿玢岩均是在伸展背景下形成的。软流圈或地幔源区物质上涌,在伸展拉张背景下底侵,导致上部地壳物质部分熔融形成了流纹岩。随后,部分起源于“混合”地幔源区的基性岩浆沿裂隙通道侵位到浅层地壳形成了辉绿玢岩岩墙。

5.3 大地构造意义

三叠纪末,随着华北地块与扬子地块沿大别-苏鲁造山带碰撞-拼合结束(陈移之等,1992; Li *et al.*, 1993, 1994; Ames *et al.*, 1996; 李曙光等,1996,1997; Hacker *et al.*, 1998; 程裕淇等,2000; 王道轩等,2001; 杨经绥等,2002; 陈道公等,2002; 刘福来等,2003),中国大陆东部在侏罗-白垩纪时期进入了构造体制转换阶段。该构造体制的转换造成了华北克拉通东部大规模的破坏,伴随着壳内强烈韧性变形以及频繁的燕山期岩浆活动等现象。例如:1)古生代期间,华北克拉通的岩石圈厚达 200km(池际尚和路凤香,1996),中生代期间,由于地幔上涌和强烈的构造-岩浆活动,快速减薄至厚度不超过 80km(Fan and Hooper, 1991; Fan and Menzies, 1992; Menzies *et al.*, 1993; 林舸等,2004);2)华北动力学体制由早中生代的南北向收缩或挤压转变为 NWW-SEE 向的板内变形与伸展背景(赵越等,2010),形成一系列断陷盆地和盆岭相间的构造格局,如:胶莱盆地、承德盆地、阜新盆地、合肥盆地等;3)大量中生代燕山期岩浆活动在中国东部广泛发育(Wu *et al.*, 2005),伴随着大规模成矿作用(Yang *et al.*, 2003; Sun *et al.*, 2007; 毛景文等,2008);4)广泛分布变质核杂岩(Davis *et al.*, 1996; Darby *et al.*, 2004; Lin *et al.*, 2011)。关于上述构造体制转换的成因机制,代表性的观点有:太平洋板块俯冲及其远程效应(Lapierre *et al.*, 1997; Qiu *et al.*, 2002; 吴福元等,2008; 朱日祥等,2011,2012; Li *et al.*, 2018);岩石圈拆沉与陆内拉张(邓晋福等,1996,2000; Gao *et al.*, 1998,2002);软流圈对岩石圈的侵蚀作用(Menzies and Xu, 1998; Xu, 2001);岩石圈置换等(翟明国和樊祺诚,2002)。

灵山岛所在的鲁东地区位于苏鲁造山带东部。侏罗-白垩纪时期,鲁东地区的岩浆活动可以划分为为三幕:1)玲珑期(160~150Ma),该时期区域构造挤压导致地壳增厚,并引起地壳重熔形成 S 型花岗岩(苗来成等,1998; 宋明春等,2009; Ma *et al.*, 2013);2)郭家岭期(135~125Ma),构造应力体制由挤压为主转向以伸展为主,形成一系列花岗闪长岩和二长花岗岩(关康等,1998; Yang *et al.*, 2014);3)崂山期(125~105Ma),广泛发育裂谷环境下的岩浆活动产物,如 I 型和 A 型花岗岩(赵广涛等,1997; Goss *et al.*, 2010; Li *et al.*, 2014),以及基性岩墙等(Guo *et al.*, 2004; Liu *et al.*, 2004,2009; Ma *et al.*, 2014)。区域上,这与华北东部在 140~110Ma 期间,地幔底侵作用最为强烈(翟明国等,2003; Wu *et al.*, 2005; 朱日祥等,2012),且构造背景由侏罗纪挤压环境转变为白垩纪伸展环境相对应(任纪舜等,1990,1998; 陈培荣等,2002; 谢桂青等,2005; 李献华等,2007; 邢光福等,2008)。此外,鲁东地区发育白垩纪由北到南的盆岭相间构造格局,亦表明了构造体制的转变(任凤楼等,2007; 张岳桥等,2008)。

本次研究的灵山岛流纹岩和辉绿玢岩的形成时代分别为 118±2Ma 和 109±3Ma,对应的岩浆活动大致处于区内崂

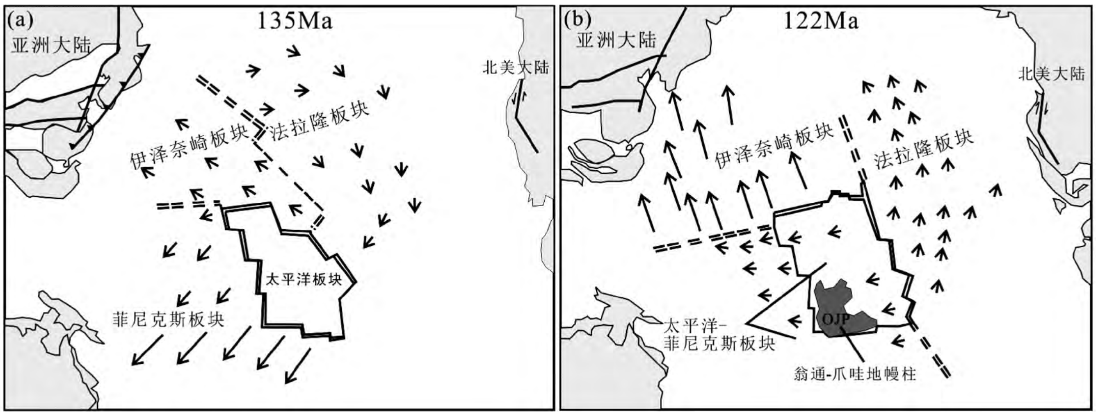

图16 早白垩世翁通-爪哇地幔柱引发古太平洋板块及其周缘各板块的相互运动关系改变(据 Ratcliff *et al.*, 1998; Goldfarb *et al.*, 2007)

Fig. 16 Early Cretaceous relative motion change of paleo-Pacific plate and its surrounding plate linked to the rise of the Ontong-Java plume (OJP) (after Ratcliff *et al.*, 1998; Goldfarb *et al.*, 2007)

山期岩浆活动期。玄武质岩浆的侵入会造成上覆地壳的伸展、拉张,岩浆沿裂隙上侵形成基性岩墙并导致上覆地壳物质部分熔融形成高钾钙碱性I型花岗岩、A型花岗岩以及对应火山岩(Windley, 1977; Halls and Fahrig, 1987; 李江海等, 1997)。如前所述,灵山岛广泛发育形成于伸展背景下的具有代表性的流纹岩和辉绿玢岩岩墙,与该时期的区域伸展构造背景对应。除灵山岛外,在胶南地区还广泛发育代表裂谷环境的碱性花岗岩(赵广涛等, 1997; 王世进等, 2010; Goss *et al.*, 2010; Li *et al.*, 2014)。再者,野外观察表明,相比于苏鲁-大别造山带内早中生代强烈的变质变形,灵山岛的岩石基本未发生变质、变形,仅局部发育同沉积构造和脆性断裂,表明灵山岛并未经历与挤压-碰撞造山相关的构造活动。因此,早白垩世晚期,灵山岛整体处于伸展拉张背景下,发育一系列断陷盆地和伸展穹窿。在侏罗-白垩纪时期,华北东部太平洋板块俯冲构造体制占据着主导地位(Xu *et al.*, 1987; Maruyama *et al.*, 1997; Wu *et al.*, 2005; Sun *et al.*, 2007; Wang *et al.*, 2011; 朱日祥等, 2012)。早白垩世(~124Ma),在南太平洋翁通-爪哇地幔柱(Ontong-Java plume)的持续作用下,古太平洋板块"捕获"了邻近的菲尼克斯板块(Phoenix plate)并导致各板块俯冲方向的改变(Ratcliff *et al.*, 1998)。其中最显著的是伊泽奈崎板块(Izanagi plate)不再受到菲尼克斯板块(Phoenix plate)SW方向的拖拽作用影响,继而由早期向东亚大陆的NW正交俯冲转向N斜交俯冲(图16a, b);同时,重组后的古太平洋板块由早期向东亚大陆SW向俯冲转向NW向俯冲。伊泽奈崎-古太平洋板块俯冲方向改变,导致华北东部由挤压转向伸展背景(Maruyama *et al.*, 1997; Goldfarb *et al.*, 2007; 孙卫东等, 2008)。因此,这些岩浆活动是白垩纪大规模的岩石圈伸展减薄和地幔上涌背景下形成的,而灵山岛当时可能处于盆地或边缘海环境,在沉积过程中伴随着强烈岩浆-火山活动。

6 结论

(1) LA-ICP-MS锆石U-Pb定年结果显示,灵山岛白色流纹岩和辉绿玢岩形成年龄为分别为118±2Ma和109±3Ma,辉绿玢岩的形成时代稍晚于流纹岩,二者属于早白垩世晚期岩浆活动产物。

(2) 锆石Hf同位素组成表明,流纹岩岩浆中结晶出的锆石具有−31.0~−24.5的$\varepsilon_{Hf}(t)$值,且锆石两阶段模式年龄远大于锆石结晶年龄,指示其来源于古老地壳物质部分熔融;辉绿玢岩岩浆中结晶出的锆石$\varepsilon_{Hf}(t)$值分别为−31.2~−28.8和+7.1~+8.1,指示其来源于有深部亏损软流圈地幔物质加入的富集地幔源区。

(3) 流纹岩与辉绿玢岩均形成于伸展拉张背景下。流纹岩是由地幔物质上涌、底侵导致地壳物质部分熔融形成的;辉绿玢岩是起源于板内地幔的部分熔融,其偏碱性的岩石化学特征、Nb和Ta无异常,以及含较高的正$\varepsilon_{Hf}(t)$值的锆石表明其具有深部地幔特征,受岩石圈地幔和软流圈地幔的影响。

(4) 灵山岛流纹岩和辉绿玢岩与华北东部普遍出露的白垩纪岩浆岩石的特点相同,都是华北克拉通岩石圈减薄的产物。

致谢 两位匿名审稿专家提出了宝贵修改意见,在此表示诚挚的感谢!

References

Albarède F, Scherer EE, Blichert-Toft J, Rosing M, Simionovici A and Bizzarro M. 2006. γ-ray irradiation in the early Solar System and the conundrum of the ^{176}Lu decay constant. Geochimica et

Cosmochimica Acta, 70(5): 1261 - 1270

Aldanmaz E, Pearce JA, Thirlwall MF and Mitchell JG. 2000. Petrogenetic evolution of Late Cenozoic, post-collision volcanism in western Anatolia, Turkey. Journal of Volcanology and Geothermal Research, 102(1 - 2): 67 - 95

Ames L, Zhou GZ and Xiong BC. 1996. Geochronology and isotopic character of ultrahigh-pressure metamorphism with implications for collision of the Sino-Korean and Yangtze cratons, Central China. Tectonics, 15(2): 472 - 489

Bao ZA, Chen L, Zong CL, Yuan HL, Chen KY and Dai MN. 2017. Development of pressed sulfide powder tablets for in situ sulfur and lead isotope measurement using LA-MC-ICP-MS. International Journal of Mass Spectrometry, 421: 255 - 262

Basu AR, Wang J, Huang WK, Xie GH and Tatsumoto M. 1991. Major element, REE, and Pb, Nd and Sr isotopic geochemistry of Cenozoic volcanic rocks of eastern China: Implications for their origin from suboceanic-type mantle reservoirs. Earth and Planetary Science Letters, 105(1 - 3): 149 - 169

Belousova EA, Griffin WL, O'Reilly SY and Fisher NI. 2002. Igneous zircon: Trace element composition as an indicator of source rock type. Contributions to Mineralogy and Petrology, 143(5): 602 - 622

Blichert-Toft J and Albarède F. 1997. The Lu-Hf isotope geochemistry of chondrites and the evolution of the mantle-crust system. Earth and Planetary Science Letters, 148(1 - 2): 243 - 258

Blichert-Toft J, Chauvel C and Albarède F. 1997. Separation of Hf and Lu for high-precision isotope analysis of rock samples by magnetic sector-multiple collector ICP-MS. Contributions to Mineralogy and Petrology, 127(3): 248 - 260

Bouvier A, Vervoort JD and Patchett PJ. 2008. The Lu-Hf and Sm-Nd isotopic composition of CHUR: Constraints from unequilibrated chondrites and implications for the bulk composition of terrestrial planets. Earth and Planetary Science Letters, 273(1 - 2): 48 - 57

Briand B, Bouchardon JL, Capiez P and Piboule M. 2002. Felsic (A-type) -basic (plume-induced) Early Palaeozoic bimodal magmatism in the Maures massif (southeastern France). Geological Magazine, 139(3): 291 - 311

Chappell BW. 1999. Aluminium saturation in I- and S-type granites and the characterization of fractionated haplogranites. Lithos, 46(3): 535 - 551

Chen DG, Deloule E, Xia QK, Wu YB and Chen H. 2002. Metamorphic zircon from Shuanghe ultra-high pressure eclogite, Dabieshan: Ion microprobe and internal micro-structure study. Acta Petrologica Sinica, 18(3): 369 - 377 (in Chinese with English abstract)

Chen PR, Hua RM, Zhang BT, Lu JJ and Fan CF. 2002. Early Yanshanian post-orogenic granitoids in the Nanling region: Petrological constraints and geodynamic settings. Science in China (Series D), 45(8): 755 - 768

Chen YZ, Li SG, Cong BL, Zhang RH and Zhang ZQ. 1992. Time and genesis of eclogites from the Jiaonan area: Evidences from Sr, Nd isotope geochemistry and chronology. Chinese Science Bulletin, 37(23): 2169 - 2172 (in Chinese)

Chen ZH, Xing GF, Jiang Y and Kuang FX. 2013. Discovery of the Paleoproterozoic A-type rhyolite porphyries in the Cathaysia Block and its geological significance. Geotectonica et Metallogenia, 37(3): 499 - 510 (in Chinese with English abstract)

Cheng YQ, Liu DY, Williams IS, Jian P, Zhuang YX and Gao TS. 2000. SHRIMP U-Pb dating of zircons of a dark-coloured eclogite and a garnet-bearing gneissic-granitic rock from Bixiling, eastern Dabie area: Isotope chronological evidence of Neoproterozoic HP-UHP metamorphism. Acta Geologica Sinica, 74(3): 193 - 205 (in Chinese with English abstract)

Chi JS and Lu FX. 1996. Characteristics of Kimberlites and Paleozoic Lithosphere Mantle in North China Plateform. Beijing: Science Press, 292 - 293 (in Chinese)

Collins WJ, Beams SD, White AJR and Chappell BW. 1982. Nature and origin of A-type granites with particular reference to southeastern Australia. Contributions to Mineralogy and Petrology, 80(2): 189 - 200

Darby BJ, Davis GA, Zhang XH, Wu FY, Wilde S and Yang JH. 2004. The newly discovered Waziyu metamorphic core complex, Yiwulü Shan, western Liaoning Province, Northwest China. Earth Science Frontiers, 11(3): 145 - 155

Davis GA, Qian XL and Zheng YD. 1996. Mesozoic Deformation and Plutonism in the Yunmeng Shan: A Chinese Metamorphic Core Complex North of Beijing, China. New York: Cambridge University Press, 253 - 280

Deng JF, Zhao HL, Mo XX, Wu ZX and Luo ZH. 1996. Continental Roots-Plume Tectonics of China: Key to the Continental Dynamics. Beijing: Geological Publishing House, 110 - 112 (in Chinese)

Deng JF, Zhao GC, Zhao HL, Luo ZH, Dai SQ and Li KM. 2000. Yanshanian igneous petrotectonic assemblage and orogenic-deep processes in East China. Geological Review, 46(1): 41 - 48 (in Chinese with English abstract)

Ding S, Huang H, Niu YL, Zhao ZD, Yu XH and Mo XX. 2011. Geochemistry, geochronology and petrogenesis of East Kunlun high Nb-Ta rhyolites. Acta Petrologica Sinica, 27(12): 3603 - 3614 (in Chinese with English abstract)

Dong XP, Lv HB, Zhang X, Zhang HC, Wang J and Zhang SJ. 2013. Stage analysis on the soft-sediment deformation in the Early Cretaceous flysch, Lingshan Island, Shandong Province. Geological Review, 59(6): 1060 - 1067 (in Chinese with English abstract)

Dong XP, Lu HB, Zhang X, Zhang HC, Wang J and Zhang SJ. 2014. Slump scarp outcrop found in Early Cretaceous flysch, north of Lingshan Island, Qingdao, Shandong. Geological Review, 60(4): 771 - 779 (in Chinese with English abstract)

Fan QC and Hooper PR. 1991. The Cenozoic basaltic rocks of eastern China: Petrology and chemical composition. Journal of Petrology, 32(4): 765 - 810

Fan WM and Menzies MA. 1992. Destruction of aged lower lithosphere and accretion of asthenosphere mantle beneath eastern China. Geotectonica et Metallogenia, 16: 171 - 180

Fan WM, Guo F, Wang YJ, Lin G and Zhang M. 2001. Post-orogenic bimodal volcanism along the Sulu orogenic belt in eastern China. Physics and Chemistry of the Earth, Part A: Solid Earth and Geodesy, 26(9 - 10): 733 - 746

Feng ZZ, Bao ZD, Zheng XJ and Wang Y. 2016. Researches of soft-sediment deformation structures and seismites in China: A brief review. Journal of Palaeogeography, 5(4): 311 - 317

Feng ZZ, Bao ZD, Zheng XJ and Wang Y. 2017. Researches of soft-sediment deformation structures and seismites in China: A brief review. Journal of Palaeogeography, 19(1): 7 - 12 (in Chinese with English abstract)

Fu GQ and Li SJ. 1984. Texture facies of submarine volcanic rocks. Geological Review, 30(4): 319 - 324 (in Chinese with English abstract)

Gao P, Zheng YF and Zhao ZF. 2016. Distinction between S-type and peraluminous I-type granites: Zircon versus whole-rock geochemistry. Lithos, 258 - 259: 77 - 91

Gao S, Zhang BR, Jin ZM, Kern H, Luo TC and Zhao ZD. 1998. How mafic is the lower continental crust? Earth and Planetary Science Letters, 161(1 - 4): 101 - 117

Gao S, Rudnick RL, Carlson RW, McDonough WF and Liu YS. 2002. Re-Os evidence for replacement of ancient mantle lithosphere beneath the North China Craton. Earth and Planetary Science Letters, 198(3 - 4): 307 - 322

Gao XC. 1991. Anaiysis of relict sediments in the area of southern Huanghai Sea near Lingshan Island and its sedimentary environment. Journal of Oceanography of Huanghai & Bohai Seas, 9(1): 51 - 55 (in Chinese with English abstract)

Ge YZ, Zhong JH, Fan XF, Ren QQ and Shao ZF. 2015. Study on internal sedimentary and structural features of the slump body in Lingshan Island, Qingdao, Shandong. Geological Review, 61(3): 634 - 644 (in Chinese with English abstract)

Goldfarb RJ, Hart CRJ, Davis G and Groves DI. 2007. East Asian gold: Deciphering the anomaly of Phanerozoic gold in Precambrian cratons.

Economic Geology, 102(3): 341-346

Goss SC, Wilde SA, Wu FY and Yang YH. 2010. The age, isotopic signature and significance of the youngest Mesozoic granitoids in the Jiaodong Terrane, Shandong Province, North China Craton. Lithos, 120(3-4): 309-326

Griffin WL, Pearson NJ, Belousova E, Jackson SE, Van Achterbergh E, O'Reilly SY and Shee SR. 2000. The Hf isotope composition of cratonic mantle: LAM-MC-ICPMs analysis of zircon megacrysts in kimberlites. Geochimica et Cosmochimica Acta, 64(1): 133-147

Griffin WL, Wang X, Jackson SE, Pearson NJ, O'Reilly SY, Xu XS and Zhou XM. 2002. Zircon chemistry and magma mixing, SE China: In-situ analysis of Hf isotopes, Tonglu and Pingtan igneous complexes. Lithos, 61(3-4): 237-269

Guan K, Luo ZK, Miao LC and Huang JZ. 1998. SHRIMP in zircon chronology for Guojialing suite granite in Jiaodong Zhaoye district. Scientia Geologica Sinica, 33(3): 318-328 (in Chinese with English abstract)

Guo F, Fan WM, Wang YJ and Lin G. 2001. Late mesozoic mafic intrusive complexes in North China Block: Constraints on the nature of subcontinental lithospheric mantle. Physics and Chemistry of the Earth, Part A: Solid Earth and Geodesy, 26(9-10): 759-771

Guo F, Fan WM, Wang YJ and Zhang M. 2004. Origin of early cretaceous calc-alkaline lamprophyres from the Sulu orogen in eastern China: Implications for enrichment processes beneath continental collisional belt. Lithos, 78(3): 291-305

Hacker BR, Ratschbacher L, Webb L, Ireland T, Walker D and Dong SW. 1998. U/Pb zircon ages constrain the architecture of the ultrahigh-pressure Qinling-Dabie Orogen, China. Earth and Planetary Science Letters, 161(1-4): 215-230

Halls HC and Fahrig WF. 1987. Mafic dyke swarms (IDC-I). Geological Association of Canada Special Papers, 34: 483-491

Hastie AR, Kerr AC, Pearce JA and Mitchell SF. 2007. Classification of altered volcanic Island arc rocks using immobile trace elements: Development of the Th-Co discrimination diagram. Journal of Petrology, 48(12): 2341-2357

Hildreth W, Hallidy AN and Christiansen RL. 1991. Isotopic and chemical evidence concerning the genesis and contamination of basaltic and rhyolitic magma beneath the Yellowstone plateau volcanic field. Journal of Petrology, 32(1): 63-138

Hirose K. 1997. Melting experiments on lherzolite KLB-1 under hydrous conditions and generation of high-magnesian andesitic melts. Geology, 25(1): 42-44

Hofmann AW, Jochum KP, Seufert M and White WM. 1986. Nb and Pb in oceanic basalts: New constraints on mantle evolution. Earth and Planetary Science Letters, 79(1-2): 33-45

Hofmann AW. 1988. Chemical differentiation of the Earth: The relationship between mantle, continental crust, and oceanic crust. Earth and Planetary Science Letters, 90(3): 297-314

Hofmann AW. 2003. Sampling mantle heterogeneity through oceanic basalts: Isotopes and trace elements. In: Holland HD and Turekian KK (eds.). Treatise on Geochemistry. Oxford: Elsevier, 61-101

Hoskin PWO and Black LP. 2000. Metamorphic zircon formation by solid-state recrystallization of protolith igneous zircon. Journal of Metamorphic Geology, 18(4): 423-439

Hoskin PWO and Schaltegger U. 2003. The composition of zircon and igneous and metamorphic petrogenesis. Reviews in Mineralogy and Geochemistry, 53(1): 27-62

Irvine TN and Baragar WRA. 1971. A guide to the chemical classification of the common volcanic rocks. Canadian Journal of Earth Sciences, 8(5): 523-548

Jung C, Jung S, Hoffer E and Berndt J. 2006. Petrogenesis of Tertiary mafic alkaline magmas in the Hocheifel, Germany. Journal of Petrology, 47(8): 1637-1671

Kerrich R, Polat A, Wyman D and Hollings P. 1999. Trace element systematics of Mg-, to Fe-tholeiitic basalt suites of the Superior Province: Implications for Archean mantle reservoirs and greenstone belt genesis. Lithos, 46(1): 163-187

Lapierre H, Jahn BM, Charvet J and Yu YW. 1997. Mesozoic felsic arc magmatism and continental olivine tholeiites in Zhejiang Province and their relationship with the tectonic activity in southeastern China. Tectonophysics, 274(4): 321-338

Le Bas MJ, Le Maitre RW, Streckeisen A and Zanettin B. 1986. A chemical classification of volcanic rocks based on the total alkali-silica diagram. Journal of Petrology, 27(3): 745-750

Li H, Ling MX, Ding X, Zhang H, Li CY, Liu DY and Sun WD. 2014. The geochemical characteristics of Haiyang A-type granite complex in Shandong, eastern China. Lithos, 200-201: 142-156

Li J, Jin AW, Hou GT, Fu WZ and Yang ZQ. 2015. Study on Early Cretaceous stress fields and geological significance of Lingshan Island. Acta Scientiarum Naturalium Universitatis Pekinensis, 51(6): 1069-1077 (in Chinese with English abstract)

Li JH, He WY and Qian XL. 1997. Genetic mechanism and tectonic setting of Proterozoic mafic dyke swarm: Its implication for paleoplate reconstruction. Geological Journal of China Universities, 3(3): 272-281 (in Chinese with English abstract)

Li SG, Xiao YL, Liu DL, Chen YZ, Ge NJ, Zhang ZQ, Sun SS, Cong BL, Zhang RY, Hart SR and Wang SS. 1993. Collision of the North China and Yangtse blocks and formation of coesite-bearing eclogites: Timing and processes. Chemical Geology, 109(1-4): 89-111

Li SG, Wang SS, Chen YZ, Liu DL, Qiu J, Zhou HX and Zhang ZM. 1994. Excess argon in phengite from eclogite: Evidence from dating of eclogite minerals by Sm-Nd, Rb-Sr and ^{40}Ar-^{39}Ar methods. Chemical Geology, 112(3-4): 343-350

Li SG, Jagouty E, Xiao YL, Ge NJ and Chen YZ. 1996. Chronology of ultrahigh-pressure metamorphism in the Dabie Mountain and Su-Lu terrane: I. Sm-Nd isotopic system. Science in China (Series D), 39(6): 597-609

Li SG, Li HM, Chen YZ, Xiao YL and Liu DL. 1997. The UHP metamorphic geochronology of Dabie-Sulu terrain-II: Zircon U-Pb isotope system. Science in China (D), 27(3): 200-206 (in Chinese)

Li SJ, Zhang XY, Zhao XL, Sun ZX, Zhang DY, Zhang L, Xu L, Wei N and Liu BM. 2017. Discovery of fish and conchostracan fossils in Lower Cretaceous in Lingshan Island, Qingdao, Shandong. Geological Review, 63(1): 1-6 (in Chinese with English abstract)

Li WP. 2011. Geochemistry characteristics of the Late Cretaceous adakitic rhyolites of Daxingzhuang Formation and its genesis in Yixian area, western Liaoning Province. Earth Science (Journal of China University of Geosciences), 36(3): 429-439 (in Chinese with English abstract)

Li XH, Zhou HW, Li ZX and Liu Y. 2002. Petrogenesis of Neoproterozoic bimodal volcanics in western Sichuan and its tectonic implications: Geochemical and Sm-Nd isotopic constraints. Chinese Journal of Geology, 37(3): 264-276 (in Chinese with English abstract)

Li XH, Li WX and Li ZX. 2007. On the genetic classification and tectonic implications of the Early Yanshanian granitoids in the Nanling range, South China. Chinese Science Bulletin, 52(14): 1873-1885

Li XY, Li SZ, Suo YH, Somerville ID, Huang F, Liu X, Wang PC, Han ZX and Jin LJ. 2018. Early Cretaceous diabases, lamprophyres and andesites-dacites in western Shandong, North China Craton: Implications for local delamination and Paleo-Pacific slab rollback. Journal of Asian Earth Sciences, 160: 426-444

Liang Z and Zhou YQ. 2017. Soft-Sediment deformation structures related to slumping in Lower Cretaceous turbidite in Lingshan Island, Shandong Province. Earth Science, 42(10): 1715-1724 (in Chinese with English abstract)

Lin G, Zhang YH, Wang YJ, Guo F, Fang WM and Yan Y. 2004. Lithospheric thinning in the North China block: A mumerical approach on thermal perturbation and tectonic extension. Geotectonica et Metallogenia, 28(1): 8-14 (in Chinese with English abstract)

Lin W, Monié P, Faure M, Schärer U, Shi YH, Le BN and Wang QC. 2011. Cooling paths of the NE China crust during the Mesozoic

extensional tectonics: Example from the South-Liaodong Peninsula metamorphic core complex. Journal of Asian Earth Sciences, 42(5): 1048－1065
Ling WL, Xie XJ, Liu XM and Cheng JP. 2006. Zircon U-Pb dating on the Mesozoic volcanic suite from the Qingshan Group stratotype section in eastern Shandong Province and its tectonic significance. Science in China (Series D), 50(6): 813－824
Ling WL, Duan RC, Xie XJ, Zhang YQ, Zhang JB, Cheng JP, Liu XM and Yang HM. 2009. Contrasting geochemistry of the Cretaceous volcanic suites in Shandong Province and its implications for the Mesozoic lower crust delamination in the eastern North China craton. Lithos, 113(3): 640－658
Liu CQ, Masuda A and Xie GH. 1994. Major- and trace-element compositions of Cenozoic basalts in eastern China: Petrogenesis and mantle source. Chemical Geology, 114(1－2): 19－42
Liu FF, Zhou YQ, Xu H and Zhang ZK. 2016. Origin of the Lingshan Island and geotectonic significance. Marine Geology Frontiers, 32(3): 33－40 (in Chinese with English abstract)
Liu FL, Xu ZQ and Song B. 2003. Determination of UHP and retrograde metamorphic ages of the Sulu Terrane: Evidence from SHRIMP U-Pb dating on zircons of gneissic rocks. Acta Geologica Sinica, 77(2): 229－237 (in Chinese with English abstract)
Liu S, Hu RZ, Zhao JH and Feng CX. 2003. Tectonic setting and petrogenesis of Qingshan Formation volcanic rocks in western Shandong Province: Evidence from major elements and trace elements. Geochimica, 32(4): 306－316 (in Chinese with English abstract)
Liu S, Hu RZ, Zhao JH and Feng CX. 2004. K-Ar geochronology of Mesozoic mafic dikes in Shandong Province, eastern China: Implications for crustal extension. Acta Geologic Sinica, 78(6): 1207－1213
Liu S, Hu RZ, Gao S, Feng CX, Yu BB, Feng GY, Qi YQ, Wang T and Coulson IM. 2009. Petrogenesis of Late Mesozoic mafic dykes in the Jiaodong Peninsula, eastern North China Craton and implications for the foundering of lower crust. Lithos, 113(3－4): 621－639
Liu S, Feng CX, Hu RZ, Zhai MG, Gao S, Lai SC, Yan J, Coulson IM and Zou HB. 2015. Zircon U-Pb geochronological, geochemical, and Sr-Nd isotope data for Early Cretaceous mafic dykes in the Tancheng-Lujiang Fault area of the Shandong Province, China: Constraints on the timing of magmatism and magma genesis. Journal of Asian Earth Sciences, 98: 247－260
Liu S, Feng CX, Zhai MG, Hu RC, Lai SC, Chen JJ and Yan J. 2016. Zircon U-Pb age, geochemical, and Sr-Nd-Hf isotopic constraints on the origin of Early Cretaceous mafic dykes from western Shandong Province, eastern North China Craton, China. Acta Petrologica Sinica, 32(3): 629－645 (in English with Chinese abstract)
Liu Y, Liu XM, Hu ZC, Diwu CR, Yuan HL and Gao S. 2007. Evaluation of accuracy and long-term stability of determination of 37 trace elements in geological samples by ICP-MS. Acta Petrologica Sinica, 23(5): 1203－1210 (in Chinese with English abstract)
Liu YS and Gao S. 2007. High Nb/Ta ratios of the Mesozoic basalts from North China: Records of continental crust recycling. Bulletin of Mineralogy, Petrology and Geochemistry, 26(1): 19－28 (in Chinese with English abstract)
Luan GZ, Li AL, Wang J, Li G and Xie RJ. 2010. The geological origin division of the main sea island in Qingdao area and environment analysis. Periodical of Ocean University of China, 40(8): 111－116 (in Chinese with English abstract)
Ludwig KR. 2003. User's Manual for Isoplot 3.00: A Geochronological Toolkit for Microsoft Excel. Berkeley, California: Berkeley Geochronology Center Special Publication, 4: 1－70
Lü HB, Wang J and Zhang HC. 2011. Discovery of the Late Mesozoic slump beds in Lingshan Island, Shandong, and a pilot research on the regional tectonics. Acta Geologica Sinica, 85(6): 938－946 (in Chinese with English abstract)
Lü HB, Zhang HC, Wang J, Zhang SJ, Dong XP and Zhang X. 2012. A giant olistolith discovered in the Late Mesozoic turbidites in Lingshan Island, Jiaonan, Shandong. Geological Review, 58(1): 80－81 (in Chinese)
Lü HB, Zhang HC, Wang J, Zhang SJ, Dong XP and Zhang X. 2013. Lingshan Island Early Cretaceous flysch not intracontinental Delta: A reply to Professor Zhong Jianhua. Geological Review, 59(1): 11－14 (in Chinese)
Ma L, Jiang SY, Dai BZ, Jiang YH, Hou ML, Pu W and Xu B. 2013. Multiple sources for the origin of Late Jurassic Linglong adakitic granite in the Shandong Peninsula, eastern China: Zircon U-Pb geochronological, geochemical and Sr-Nd-Hf isotopic evidence. Lithos, 162－163: 251－263
Ma L, Jiang SY, Hofmann AW, Dai BZ, Hou ML, Zhao KD, Chen LH, Li JW and Jiang YH. 2014. Lithospheric and asthenospheric sources of lamprophyres in the Jiaodong Peninsula: A consequence of rapid lithospheric thinning beneath the North China Craton? Geochim et Cosmochimica Acta, 124: 250－271
Maniar PD and Piccoli PM. 1989. Tectonic discrimination of granitoids. GSA Bulletin, 101(5): 635－643
Mao JW, Xie GQ, Guo CL, Yuan SD, Cheng YB and Chen YC. 2008. Spatial-temporal distribution of Mesozoic ore deposits in South China and their metallogenic settings. Geological Journal of China Universities, 14(4): 510－526 (in Chinese with English abstract)
Maruyama S, Isozak Y, Kimra G and Terabayashi M. 1997. Paleogeographic maps of the Japanese Islands: Plate tectonic synthesis from 750Ma to the present. Island Arc, 6(1): 121－142
McCulloch MT, Kyser TK, Woodhead JD and Kinsley L. 1994. Pb-Sr-Nd-O isotopic constraints on the origin of rhyolites from the Taupo Volcanic Zone of New Zealand: Evidence for assimilation followed by fractionation from basalt. Contributions to Mineralogy and Petrology, 115(3): 303－312
Menzies MA, Fan WM and Zhang M. 1993. Palaeozoic and Cenozoic lithoprobes and the loss of >120km of Archaean lithosphere, Sino-Korean craton, China. In: Prichard HM, Alabaster T, Harris NBW and Neary CR (eds.). Magmatic Processes and Plate Tectonics. Geological Society, London, Special Publications, 76(1): 71－81
Menzies MA and Xu YG. 1998. Geodynamics of the North China Craton. In: Flower MFJ, Chung SL, Lo CH and Lee TY (eds.). Mantle Dynamics and Plate Interactions in East Asia. Washington, DC: American Geophysical Union Monograph, 127－154
Meschede M. 1986. A method of discriminating between different types of mid-ocean ridge basalts and continental tholeiites with the Nb-Zr-Y diagram. Chemical Geology, 56(3－4): 207－218
Middlemost EAK. 1985. Magmas and Magmatic Rocks: An Introduction to Igneous Petrology. London: Longman Group, 1－266
Miao LC, Luo ZK, Guan K and Huang JZ. 1998. The implication of the SHRIMP U-Pb age in zircon to the petrogenesis of the Linglong granite, East Shangdong Province. Acta Petrologica Sinica, 14(2): 198－206 (in Chinese with English abstract)
Patchett PJ and Tatsumoto M. 1981. A routine high-precision method for Lu-Hf isotope geochemistry and chronology. Contributions to Mineralogy and Petrology, 75(3): 263－267
Pearce JA and Cann JR. 1973. Tectonic setting of basic volcanic rocks determined using trace element analyses. Earth and Planetary Science Letters, 19(2): 290－300
Pearce JA and Norry MJ. 1979. Petrogenetic implications of Ti, Zr, Y, and Nb variations in volcanic rocks. Contributions to Mineralogy and Petrology, 69(1): 33－47
Pearce JA and Stern RJ. 2006. Origin of back-arc basin magmas: Trace element and isotope perspectives. In: Christie CR, Fisher CR, Lee SM and Givens S (eds.). Back-arc Spreading Systems: Geological, Biological, Chemical, and Physical Interactions. Washington: American Geophysical Union, 63－86
Pearce JA. 2008. Geochemical fingerprinting of oceanic basalts with applications to ophiolite classification and the search for Archean oceanic crust. Lithos, 100(1－4): 14－48
Peccerillo A and Taylor SR. 1976. Geochemistry of Eocene calc-alkaline volcanic rocks from the Kastamonu area, and Northern Turkey. Contributions Mineral and Petrology, 58(1): 63－81
Peng ZC, Zartman RE, Futa K and Chen DG. 1986. Pb-, Sr- and Nd-

isotopic systematics and chemical characteristics of Cenozoic basalts, eastern China. Chemical Geology, 59: 3 – 33

Qiu JS, Wang DZ, Lo QH and Liu H. 2001. ^{40}Ar-^{39}Ar dating for volcanic rocks of Qingshan Formation in Jiaolai Basin, eastern Shandong Province: A case study of the Fenlingshan volcanic apparatus in Wulian County. Geological Journal of China Universities, 7(3): 351 – 355 (in Chinese with English abstract)

Qiu JS, Xu XS and Lo CH. 2002a. Potash-rich volcanic rocks and lamprophyres in western Shandong Province: ^{40}Ar-^{39}Ar dating and source tracing. Chinese Science Bulletin, 47(2): 91 – 99

Qiu JS, Jiang SY, Zhang XL and Hu J. 2004. Petrogenesis of K-rich volcanic rocks on the northern and southern sides of the Dabie-Sulu orogenic belt, eastern China: Constraints from trace elements and Sr-Nd-Pb isotopes. Acta Geoscientia Sinica, 25(2): 255 – 262 (in Chinese with English abstract)

Qiu JS, Liu L and Li YL. 2012. Geochronology and geochemistry of potassic and sodic volcanic rocks in Tangtou basin, Shandong Province: Implications for lithospheric thinning beneath the North China Craton. Acta Petrologica Sinica, 28(4): 1044 – 1056 (in Chinese with English abstract)

Qiu LG, Ren FL, Cao ZX and Zhang YQ. 2008. Late Mesozoic magmatic activities and their constraints on geotectonics of Jiaodong region. Geotectonica et Metallogenia, 32(1): 117 – 123 (in Chinese with English abstract)

Qiu YM, Groves DI, McNaughton NJ, Wang LG and Zhou TH. 2002b. Nature, age, and tectonic setting of granitoid-hosted, orogenic gold deposits of the Jiaodong Peninsula, eastern North China craton, China. Mineralium Deposita, 37(3 – 4): 283 – 305

Ratcliff JT, Bercovici D, Schubert G and Kroenke LW. 1998. Mantle plume heads and the initiation of plate tectonic reorganizations. Earth and Planetary Science Letters, 156(3 – 4): 195 – 207

Ren FL, Zhang YQ, Qiu LG, Liu ZQ and Wang DH. 2007. Evolution of the structural stress field in Jiaolai basin in Cretaceous. Geotectonica et Metallogenia, 31(2): 157 – 167 (in Chinese with English abstract)

Ren JS, Chen TY, Niu BG, Liu ZG and Liu FR. 1990. Lithospheric Tectonic Evolution and Mineralization in Eastern China and Adjacent Areas. Beijing: Science Press, 1 – 205 (in Chinese)

Ren JS, Niu BG, He ZJ, Xie GL and Liu ZG. 1998. Tectonic framework and dynamic evolution of eastern China. In: Ren JS and Yang WR (eds.). Lithosphere Framework and Tectonic-Magma Evolution of Eastern China. Beijing: Atomic Energy Publication, 1 – 12 (in Chinese)

Rudnick RL and Gao S. 2003. Composition of the continental crust. In: Rudnick RL (ed.). Treatise on Geochemistry. Amsterdam: Elsevier, 3: 1 – 64

Shangdong Provincial No. 4 Institute of Geological and Mineral Survey. 2003. Regional Geology in Shandong Province. Jinan: Shandong Cartographic Publishing House, 1 – 970 (in Chinese)

Shao ZF, Zhong JH, Li Y, Mao C, Liu SX, Ni LT, Tian Y, Cui XY, Liu YT, Wang XN, Li WH and Ling GS. 2014a. Characteristics and sedimentary processes of lamina-controlled sand-particle imbricate structure in deposits on Lingshan Island, Qingdao, China. Science China (Earth Sciences), 57(5): 1061 – 1076

Shao ZF, Zhong JH, Li Y, Ni LT, Liu SX, Fan LH and Chen B. 2014b. The sedimentary characteristics and environmental analysis of Late Mesozoic gravity flows in Lingshan Island. Geological Review, 60(3): 555 – 566 (in Chinese with English abstract)

Shervais JW. 1982. Ti-V plots and the petrogenesis of modern and ophiolitic lavas. Earth and Planetary Science Letters, 59(1): 101 – 118

Shinjo R and Kato Y. 2000. Geochemical constraints on the origin of bimodal magmatism at the Okinawa Trough, an incipient back-arc basin. Lithos, 54(3 – 4): 117 – 137

Song MC, Xu JX, Wang PC, Cui SX, Huang TL and Liu MW. 2009. Pattern and Evolution of Geotexture, Shandong Province. Beijing: Geological Publishing House, 36 – 37 (in Chinese)

Sun SS and McDonough WF. 1989. Chemical and isotopic systematics of oceanic basalts: Implications for mantle composition and processes. In: Saunders AD and Norry MJ (eds.). Magmatism in the Ocean Basins. Geological Society, London, Special Publication, 42(1): 313 – 345

Sun WD, Ding X, Hu YH and Li XH. 2007. The golden transformation of the Cretaceous plate subduction in the west Pacific. Earth and Planet Science Letter, 262(3 – 4): 533 – 542

Sun WD, Ling MX, Wang FY, Ding X, Hu YH, Zhou JB and Yang XY. 2008. Pacific plate subduction and Mesozoic geological event in eastern China. Bulletin of Mineralogy, Petrology and Geochemistry, 27(3): 218 – 225 (in Chinese with English abstract)

Sylvester PJ. 1989. Post-collisional alkaline granites. The Journal of Geology, 97(3): 261 – 280

Tang JF, Liu YL and Wang QF. 2008. Geochronology of Mesozoic volcanic rocks in Shandong Province. Acta Petrologica Sinica, 24(6): 1333 – 1338 (in Chinese with English abstract)

Thirlwall MF and Anczkiewicz R. 2004. Multidynamic isotope ratio analysis using MC-ICP-MS and the causes of secular drift in Hf, Nd and Pb isotope ratios. International Journal of Mass Spectrometry, 235(1): 59 – 81

Turner S, Sandiford M and Foden J. 1992. Some geodynamic and compositional constraints on "postorogenic" magmatism. Geology, 20(10): 931 – 934

Uyeda S and Miyashiro A. 1974. Plate tectonics and the Japanese Islands: A synthesis. GSA Bulletin, 85(7): 1159 – 1170

Wang AD, Zhou YQ, Yan H, Wang R, Zhang ZK and Wang ZY. 2013. Characteristics of soft-sediment deformation structures of the Early Cretaceous in Lingshan Island of Shandong Province. Journal of Palaeogeography, 15(5): 718 – 728 (in Chinese with English abstract)

Wang DX, Liu Y, Li SY and Jin FQ. 2002. Lower time limit on the UHPM rock exhumation: Discovery of eclogite pebbles in the Late Jurassic conglomerates from the northern foot of the Dabie Mountains, eastern China. Chinese Science Bulletin, 47(3): 231 – 235

Wang DZ, Zhou JC, Qiu JS and Zhang HJ. 1994. The Magma mixing in Early Cretaceous volcanic activities and evidence for crust-mantle interaction in southeastern coast of China. Journal of Nanjing University (Earth Science), 6(4): 317 – 325 (in Chinese)

Wang J, Chang SC, Lu HB and Zhang HC. 2014. Detrital zircon U-Pb age constraints on Cretaceous sedimentary rocks of Lingshan Island and implications for tectonic evolution of eastern Shandong, North China. Journal of Asian Earth Sciences, 96: 27 – 45

Wang SJ, Wan YS, Wang W, Song ZY, Wang JG, Dong CY, Xie HQ and Liu QD. 2010. Forming ages of granites in Laoshan area of Shandong Province: Zircon SHRIMP U-Pb dating. Land and Resources in Shandong Province, 26(10): 1 – 5, 10 (in Chinese with English abstract)

Wang T, Zheng YD, Zhang JJ, Zeng LS, Donskaya T, Guo L and Li JB. 2011. Pattern and kinematic polarity of Late Mesozoic extension in continental NE Asia: Perspectives from metamorphic core complexes. Tectonics, 30(6): TC6007

Watson EB and Harrison TM. 1983. Zircon saturation revisited: Temperature and composition effects in a variety of crustal magma types. Earth and Planetary Science Letters, 64(2): 295 – 304

Whalen JB, Currie KL and Chappell BW. 1987. A-type granites: Geochemical characteristics, discrimination and petrogenesis. Contributions to Mineralogy and Petrology, 95(4): 407 – 419

Wilkinson JFG. 1982. The genesis of mid-ocean ridge basalt. Earth-Science Reviews, 18(1): 1 – 57

Winchester JA and Floyd PA. 1977. Geochemical discrimination of different magma series and their differentiation products using immobile elements. Chemical Geology, 20: 325 – 343

Windley BF. 1977. The Evolving Continents. New York: John Wiley and Sons, 68 – 218

Wu FY and Sun DY. 1999. The Mesozoic magmatism and lithospheric thinning in eastern China. Journal of Changchun University of Science and Technology, 29(4): 313 – 318 (in Chinese with

English abstract)

Wu FY, Sun DY, Li HM, Jahn BM and Wilde SA. 2002. A-type granites in northeastern China: Age and geochemical constraints on their petrogenesis. Chemical Geology, 187(1-2): 143-173

Wu FY, Lin JQ, Wilde SA, Zhang XQ and Yang JH. 2005. Nature and significance of the Early Cretaceous giant igneous event in eastern China. Earth and Planetary Science Letters, 233(1-2): 103-119

Wu FY, Li XH, Yang JH and Zheng YF. 2007a. Discussions on the petrogenesis of granites. Acta Petrologica Sinica, 23(6): 1217-1238 (in Chinese with English abstract)

Wu FY, Li XH, Zheng YF and Gao S. 2007b. Lu-Hf isotopic systematics and their applications in petrology. Acta Petrologica Sinica, 23(2): 185-220 (in Chinese with English abstract)

Wu FY, Xu YG, Gao S and Zheng JP. 2008. Lithospheric thinning and destruction of the North China Craton. Acta Petrologica Sinica, 24(6): 1145-1174 (in Chinese with English abstract)

Wu FY, Liu XC, Ji WQ, Wang JM and Yang L. 2017. Highly fractionated granites: Recognition and research. Science China (Earth Sciences), 60(7): 1201-1219

Xie GQ, Mao JW, Hu RZ, Li RL and Cao JJ. 2005. Discussion on some problems of Mesozoic and Cenozoic geodynamics of Southeast China. Geological Review, 51(6): 613-620 (in Chinese with English abstract)

Xing GF, Lu QD, Chen R, Zhang ZY, Nie TC, Li LM, Huang JL and Lin M. 2008. Study on the ending time of Late Mesozoic tectonic regime transition in South China: Comparing to the Yanshan area in North China. Acta Geologica Sinica, 82(4): 451-463 (in Chinese with English abstract)

Xiong XL, Adam J and Green TH. 2005. Rutile stability and rutile/melt HFSE partitioning during partial melting of hydrous basalt: Implications for TTG genesis. Chemical Geology, 218(3-4): 339-359

Xu JW, Zhu G, Tong WX, Kerei C and Liu Q. 1987. Formation and evolution of the Tancheng-Lujiang wrench fault system: A major shear system to the northwest of the Pacific Ocean. Tectonophysics, 134(4): 273-310

Xu YG. 2001. Thermo-tectonic destruction of the Archaean lithospheric keel beneath the Sino-Korean Craton in China: Evidence, timing and mechanism. Physics and Chemistry of the Earth, Part A: Solid Earth and Geodesy, 26(9-10): 747-757

Yan J, Chen JF and Xu XS. 2008. Geochemistry of Cretaceous mafic rocks from the Lower Yangtze region, eastern China: Characteristics and evolution of the lithospheric mantle. Journal of Asian Earth Sciences, 33(3-4): 177-193

Yang JH, Wu FY and Wilde SA. 2003. A review of the geodynamic setting of large-scale Late Mesozoic gold mineralization in the North China Craton: An association with lithospheric thinning. Ore Geology Review, 23(3-4): 125-152

Yang JH, Wu FY, Chung SL, Wilde SA and Chu MF. 2006. A hybrid origin for the Qianshan A-type granite, Northeast China: Geochemical and Sr-Nd-Hf isotopic evidence. Lithos, 89(1-2): 89-106

Yang JH, Wu FY, Wilde SA, Belousova E and Griffin WL. 2008. Mesozoic decratonization of the North China block. Geology, 36(6): 467-470

Yang JS, Xu ZQ, Wu CL, Liu FL, Shi RD, Wooden J and Maruyama S. 2002. SHRIMP U-Pb dating on coesite-bearing zircon: Evidence for Indosinian ultrahigh-pressure metamorphism in Su-Lu, East China. Acta Geologica Sinica, 76(3): 354-372 (in Chinese with English abstract)

Yang QY, Santosh M, Shen JF and Li SR. 2014. Juvenile vs. recycled crust in NE China: Zircon U-Pb geochronology, Hf isotope and an integrated model for Mesozoic gold mineralization in the Jiaodong Peninsula. Gondwana Research, 25(4): 1445-1468

Yang RC and Van Loon AJ. 2016. Early Cretaceous slumps and turbidites with peculiar soft-sediment deformation structures on Lingshan Island (Qingdao, China) indicating a tensional tectonic regime. Journal of Asian Earth Sciences, 129: 206-219

Yu JH, Wang DZ and Geng JH. 1998. A palaeoproterozoic A-type rhyolite. Geochimica, 27(6): 549-558 (in Chinese with English abstract)

Yuan HL, Gao S, Dai MN, Zong CL, Günther D, Fontaine GH, Liu XM and Diwu CR. 2008. Simultaneous determinations of U-Pb age, Hf isotopes and trace element compositions of zircon by excimer laser-ablation quadrupole and multiple-collector ICP-MS. Chemical Geology, 247(1-2): 100-118

Zhai MG and Fan QC. 2002. Mesozoic replacement of bottom crust in North China Craton: Anorogenic mantle-crust interaction. Acta Geologica Sinica, 18(1): 1-8 (in Chinese with English abstract)

Zhai MG, Zhu RX, Liu JM, Meng QR, Hou QL, Hu SB, Liu W, Li Z and Zhang HF. 2003. Time range of Mesozoic tectonic regime inversion in eastern North China Block. Science in China (Series D), 47(2): 151-159

Zhai MG, Fang HR, Yang JH and Miao LC. 2004. Large-scale cluster of gold deposits in East Shandong: Anorogenic metallogenesis. Earth Science Frontiers, 11(1): 85-98 (in Chinese with English abstract)

Zhai MG and Santosh M. 2013. Metallogeny of the North China Craton: Link with secular changes in the evolving Earth. Gondwana Research, 24(1): 275-297

Zhang FX, Zhou YQ, Wang AD and Yu SS. 2015. Load structures and ball-and-pillow structures on the Lingshan Island, Shandong. Sedimentary Geology and Tethyan Geology, 35(3): 42-50 (in Chinese with English abstract)

Zhang HC, Lü HB, Li JG, Wang J, Zhang SJ, Dong XP, Zhang X, Huang ZC, Shu YC and Ren XM. 2013. The Lingshandao Formation: A new lithostratigraphic unit of the Early Cretaceous in Qingdao, Shandong, China. Journal of Stratigraphy, 37(2): 216-222 (in Chinese with English abstract)

Zhang HF, Sun M, Zhou XH, Zhou MF, Fang WM and Zheng JP. 2003. Secular evolution of the lithosphere beneath the eastern North China Craton: Evidence from Mesozoic basalts and high-Mg andesites. Geochimica et Cosmochimica Acta, 67(22): 4373-4387

Zhang HF, Sun M, Zhou XH and Ying JF. 2005. Geochemical constraints on the origin of Mesozoic alkaline intrusive complexes from the North China Craton and tectonic implications. Lithos, 81(1-4): 297-317

Zhang Q, Wang Y and Wang YL. 2001. Preliminary study on the components of the lower crust in East China Plateau during Yanshanian Period: Constraints on Sr and Nd isotopic compositions of adakite-like rocks. Acta Petrologica Sinica, 17(4): 505-513 (in Chinese with English abstract)

Zhang X, Lu HB, Zhang HC, Wang J, Zhang SJ, Dong XP, Huang ZC and Shu YC. 2012. Geological significance of Early Cretaceous molasses from Lingshan Island, Jiaonan, Shandong. Qingdao: National Symposium on Palaeogeography and Sedimentology (NCPS), 159-160 (in Chinese)

Zhang YQ. 2006. Sedimentary-magmatic-tectonic evolution sequence of the Jiaolai Basin, Shangdong: Constraints on the Late Mesozoic lithospheric thinning in eastern China. Nanjing: National Symposium on Petrology and Geodynamics (abstract), 44-46 (in Chinese)

Zhang YQ, Li JL, Zhang T, Dong SW and Yuan JY. 2008. Cretaceous to Paleocene tectono-sedimentary evolution of the Jiaolai basin and the contiguous areas of the Shandong Peninsula (North China) and its geodynamic implications. Acta Geologica Sinica, 82(9): 1229-1257 (in Chinese with English abstract)

Zhang ZK, Zhou YQ, Liang WD, Yue HW, Zhou PF and Peng TM. 2016. Early Cretaceous tectonic evolution of Lingshan Island in Shandong Province and its geologic significance. Marine Geology Frontiers, 32(4): 1-10 (in Chinese with English abstract)

Zhang ZK, Zhou YQ, Peng TM, Yu SS, Yue HW, Zhou TF and Liu JZ. 2017. Geochemical characteristics and signatures of siltstones from Laiyang Group at Lingshan Island, Qingdao, Shandong. Earth Science, 42(3): 357-377 (in Chinese with English abstract)

Zhao GT, Cao QC, Wang DZ and Li HM. 1997. Zirconic U-Pb dating on

the Laoshan granitoids and its significance. Journal of Ocean University of Qingdao, 27(3): 382–388 (in Chinese with English abstract)
Zhao JH and Zhou MF. 2007. Geochemistry of Neoproterozoic mafic intrusions in the Panzhihua district (Sichuan Province, SW China): Implications for subduction-related metasomatism in the upper mantle. Precambrian Research, 152(1–2): 27–47
Zhao Y, Chen B, Zhang SH, Liu JM, Hu JM, Liu J and Pei JL. 2010. Pre-Yanshanian geological events in the northern margin of the North China Craton and its adjacent areas. Geology in China, 37(4): 900–915 (in Chinese with English abstract)
Zhong JH. 2012. Lingshan Island Mesozoic sedimentary rocks in deep water far source turbidite or continental delta deposits? A discussion with Professor Lu Hongbo. Geological Review, 58(6): 1180–1182 (in Chinese)
Zhong JH, Ni LT, Shao ZF, Li Y, Liu X, Mao C, Liu SX, Sun NL, Chen B, Wang K, Luo K, Wang SJ, Liu C, Liu B and Xiong ZQ. 2016. Tempestites and storm deposites in the Lower Cretaceous from Lingshan Island, Qingdao. Journal of Palaeogeography, 18(3): 381–398 (in Chinese with English abstract)
Zhou TH and Lü GX. 2000. Tectonics, granitoids and Mesozoic gold deposits in East Shandong, China. Ore Geology Reviews, 16(1–2): 71–90
Zhou XH. 2009. Major transformation of subcontinental lithosphere beneath North China in Cenozoic-Mesozoic: Revisited. Geological Journal of China Universities, 15(1): 1–18 (in Chinese with English abstract)
Zhou YQ, Zhang ZK, Xu H, Wang AD, Wei K, Zhang YC, Wang ZY, Li D, Chen YZ, Liu Y, Yu SS and Gao XJ. 2015a. Soft-sediment deformation structures in the sediments at Lingshan Island. Marine Geology Frontiers, 31(4): 42–54 (in Chinese with English abstract)
Zhou YQ, Zhang ZK, Liang WD, Li S and Yue HW. 2015b. Late Mesozoic tectono-magmatic activities and prototype basin restoration in eastern Shandong Province, China. Erath Science Frontiers, 22(1): 137–156 (in Chinese with English abstract)
Zhou YQ, Zhou TF, Zhang ZK, Liang Z, Liang WD, Wang AD and Yu SS. 2017. Characteristics and formation mechanism of soft-sediment deformation structures related to volcanic earthquakes of the Lower Cretaceous Qingshan Group in Lingshan Island, Shandong Province. Journal of Palaeogeography, 19(4): 567–582 (in Chinese with English abstract)
Zhu RX, Chen L, Wu FY and Liu JL. 2011. Timing, scale and mechanism of the destruction of the North China Craton. Science China (Earth Sciences), 54(6): 789–797
Zhu RX, Xu YG, Zhu G, Zhang HF, Xia QK and Zheng TY. 2012. Destruction of the North China Craton. Science China (Earth Sciences), 55(10): 1565–1587

附中文参考文献

陈道公，Deloule E，夏群科，吴元保，程昊. 2002. 大别山双河超高压榴辉岩中变质锆石：离子探针和微区结构研究. 岩石学报，18(3)：369–377
陈培荣，华仁民，章邦桐，陆建军，范春方. 2002. 南岭燕山早期后造山花岗岩类：岩石学制约和地球动力学背景. 中国科学(D辑)，32(4)：279–289
陈移之，李曙光，丛柏林，张儒缓，张宗清. 1992. 胶南榴辉岩的形成时代及成因——Sr，Nd同位素地球化学及年代学证据. 科学通报，37(23)：2169–2172
陈志洪，邢光福，姜杨，匡福祥. 2013. 华夏陆块古元古代A型流纹斑岩的发现及其地质意义. 大地构造与成矿学，37(3)：499–510
程裕淇，刘敦一，Williams IS，简平，庄育勋，高天山. 2000. 大别山碧溪岭深色榴辉岩和片麻状花岗质岩石SHRIMP分析——晋宁期高压-超高压变质作用的同位素年代学依据. 地质学报，74(3)：193–205
池际尚，路凤香. 1996. 华北地台金伯利岩及古生代岩石圈地幔特征. 北京：科学出版社，292–293
邓晋福，赵海玲，莫宣学，吴宗絮，罗照华. 1996. 中国大陆根-柱构造——大陆动力学的钥匙. 北京：地质出版社，110–112
邓晋福，赵国春，赵海岭，罗照华，戴圣潜，李凯明. 2000. 中国东部燕山期火成岩构造组合与造山-深部过程. 地质论评，46(1)：41–48
丁烁，黄慧，牛耀龄，赵志丹，喻学惠，莫宣学. 2011. 东昆仑高Nb-Ta流纹岩的年代学、地球化学及成因. 岩石学报，27(12)：3603–3614
董晓朋，吕洪波，张星，张海春，王俊，张素菁. 2013. 山东灵山岛早白垩世复理石软沉积物变形期次解析. 地质论评，59(6)：1060–1067
董晓朋，吕洪波，张星，张海春，王俊，张素菁. 2014. 灵山岛北端早白垩世复理石中的滑塌断崖. 地质论评，60(4)：771–779
冯增昭，鲍志东，郑秀娟，王媛. 2017. 中国软沉积物变形构造及地震岩研究简评. 古地理学报，19(1)：7–12
富公勤，李树钧. 1984. 海相火山岩结构相. 地质论评，30(4)：319–324
高兴辰. 1991. 南黄海灵山岛附近残留沉积及其沉积环境分析. 黄渤海海洋，9(1)：51–55
葛毓柱，钟建华，樊晓芳，任启强，邵珠福. 2015. 山东灵山岛滑塌体内部沉积及构造特征研究. 地质论评，61(3)：634–644
关康，罗镇宽，苗来成，黄佳展. 1998. 胶东招掖郭家岭型花岗岩锆石SHRIMP年代学研究. 地质科学，33(3)：318–328
李杰，金爱文，侯贵廷，付文昭，杨志强. 2015. 灵山岛早白垩世构造应力解析及区域地质意义. 北京大学学报(自然科学版)，51(6)：1069–1077
李江海，何文渊，钱祥麟. 1997. 元古代基性岩墙群的成因机制、构造背景及其古板块再造意义. 高校地质学报，3(3)：272–281
李曙光，Jagouty E，肖益林，葛宁洁，陈移之. 1996. 大别山-苏鲁地体超高压变质年代学——Ⅰ. Sm-Nd同位素体系. 中国科学(D辑)，26(3)：249–257
李曙光，李惠民，陈移之，肖益林，刘德良. 1997. 大别山-苏鲁地体超高压变质年代学——Ⅱ. 锆石U-Pb同位素体系. 中国科学(D辑)，27(3)：200–206
李守军，张祥玉，赵秀丽，孙智新，张道元，章磊，徐磊，魏宁，刘宝梅. 2017. 山东省青岛市灵山岛下白垩统中发现鱼类和叶肢介化石. 地质论评，63(1)：1–6
李伍平. 2011. 辽西义县晚白垩世大兴庄组流纹岩的地球化学特征及其成因. 地球科学—中国地质大学学报，36(3)：429–439
李献华，周汉文，李正祥，刘颖. 2002. 川西新元古代双峰式火山岩成因的微量元素和Sm-Nd同位素制约及其大地构造意义. 地质科学，37(3)：264–276
李献华，李武显，李正祥. 2007. 再论南岭燕山早期花岗岩的成因类型与构造意义. 科学通报，52(9)：981–991
梁钊，周瑶琪. 2017. 山东省灵山岛下白垩统浊积岩中与滑塌作用相关的软沉积物变形构造. 地球科学，42(10)：1715–1724

林舸，Zhang YH，王岳军，郭锋，范蔚茗，阎义．2004．华北陆块岩石圈减薄作用：热薄化与机械拉伸的数值模拟研究．大地构造与成矿学，28(1)：8－14
凌文黎，谢先军，柳小明，程建萍．2006．鲁东中生代标准剖面青山群火山岩锆石 U-Pb 年龄及其构造意义．中国科学(D辑)，36(5)：401－411
刘菲菲，周瑶琪，许红，张振凯．2016．灵山岛成因特征、类型及其地质构造意义．海洋地质前沿，32(3)：33－40
刘福来，许志琴，宋彪．2003．苏鲁地体超高压和退变质时代的厘定：来自片麻岩锆石微区 SHRIMP U-Pb 定年的证据．地质学报，77(2)：229－237
刘燊，胡瑞忠，赵军红，冯彩霞．2003．鲁西青山组火山岩形成的构造背景及其成因探讨：主元素和微量元素证据．地球化学，32(4)：306－316
刘燊，冯彩霞，翟明国，胡瑞忠，赖绍聪，陈俊瑾，颜军．2016．华北克拉通东部鲁西早白垩纪基性岩墙成因：来自锆石年龄、地球化学和 Sr-Nd-Hf 同位素的证据．岩石学报，32(3)：629－645
刘晔，柳小明，胡兆初，第五春荣，袁洪林，高山．2007．ICP-MS 测定地质样品中 37 个元素的准确度和长期稳定性分析．岩石学报，23(5)：1203－1210
刘勇胜，高山．2007．华北地区中生代玄武岩高 Nb/Ta 值对地壳岩石再循环的直接记录．矿物岩石地球化学通报，26(1)：19－28
栾光忠，李安龙，王建，李甘，谢汝吉．2010．青岛主要海岛成因分类及其地质环境分析．中国海洋大学学报，40(8)：111－116
吕洪波，王俊，张海春．2011．山东灵山岛晚中生代滑塌沉积层的发现及区域构造意义初探．地质学报，85(6)：938－946
吕洪波，张海春，王俊，张素菁，董晓朋，张星．2012．山东胶南灵山岛晚中生代浊积岩中发现巨大滑积岩块．地质论评，58(1)：80－81
吕洪波，张海春，王俊，张素菁，董晓朋，张星．2013．灵山岛早白垩世复理石不是陆内三角洲沉积-答钟建华教授．地质论评，59(1)：11－14
毛景文，谢桂青，郭春丽，袁顺达，程彦博，陈毓川．2008．华南地区中生代主要金属矿床时空分布规律和成矿环境．高校地质学报，14(4)：510－526
苗来成，罗镇宽，关康，黄佳展．1998．玲珑花岗岩中锆石的离子质谱 U-Pb 年龄及其岩石学意义．岩石学报，14(2)：198－206
邱检生，王德滋，罗清华，刘洪．2001．鲁东胶莱盆地青山组火山岩的 ^{40}Ar-^{39}Ar 定年-以五莲分岭山火山机构为例．高校地质学报，7(3)：351－355
邱检生，蒋少涌，张晓琳，胡建．2004．大别-苏鲁造山带南北两侧晚中生代富钾火山岩的成因：微量元素及 Sr-Nd-Pb 同位素制约．地球学报，25(2)：255－262
邱检生，刘亮，李友连．2012．山东汤头盆地钾质及钠质火山岩的年代学与地球化学：对华北克拉通岩石圈减薄的启示．岩石学报，28(4)：1044－1056
邱连贵，任凤楼，曹忠祥，张岳桥．2008．胶东地区晚中生代岩浆活动及对大地构造的制约．大地构造与成矿学，32(1)：117－123
任凤楼，张岳桥，邱连贵，柳忠泉，王大华．2007．胶莱盆地白垩纪构造应力场与转换机制．大地构造与成矿学，31(2)：157－167
任纪舜，陈廷愚，牛宝贵，刘志刚，刘凤仁．1990．中国东部及邻区大陆岩石圈的构造演化与成矿．北京：科学出版社，1－205
任纪舜，牛宝贵，和政军，谢广连，刘志刚．1998．中国东部的构造格局和动力演化．见：任纪舜，杨巍然编．中国东部岩石圈结构与构造岩浆演化．北京：原子能出版社，1－12
山东省第四地质矿产勘查院．2003．山东省区域地质．济南：山东省地图出版社，1－970
邵珠福，钟建华，李勇，毛毳，刘圣鑫，倪良田，田媛，刘云田，崔新颖，王晓楠，李伟华，林刚山．2014a．青岛灵山岛纹层控制的砂级颗粒支撑叠瓦构造的发现及其意义．中国科学(地球科学)，44(8)：1761－1776
邵珠福，钟建华，李勇，倪良田，刘圣鑫，范莉红，陈彬．2014b．青岛灵山岛晚中生代重力流沉积特征及环境分析．地质论评，60(3)：555－566
宋明春，徐军祥，王沛成，崔书学，黄太岭，刘明渭．2009．山东省大地构造格局和地质构造演化．北京：地质出版社，36－37
孙卫东，凌明星，汪方跃，丁兴，胡艳华，周继彬，杨晓勇．2008．太平洋板块俯冲与中国东部中生代地质事件．矿物岩石地球化学通报，27(3)：218－225
唐嘉锋，刘玉琳，王启飞．2008．山东中生代火山岩年代学研究．岩石学报，24(6)：1333－1338
王安东，周瑶琪，闫华，王瑞，张振凯，王子阳．2013．山东省灵山岛早白垩世软沉积物变形构造特征．古地理学报，15(5)：718－728
王道轩，刘因，李双应，金福全．2001．大别超高压变质岩折返至地表的时间下限：大别山北麓晚侏罗世砾岩中发现榴辉岩砾岩．科学通报，46(14)：1216－1220
王德滋，周金城，邱检生，张海进．1994．东南沿海早白垩世火山活动中的岩浆混合及壳幔作用证据．南京大学学报(地球科学)，6(4)：317－325
王世进，万渝生，王伟，宋志勇，王金光，董春艳，颉颃强，刘清德．2010．山东崂山花岗岩形成时代-锆石 SHRIMP U-Pb 定年．山东国土资源，26(10)：1－5，10
吴福元，孙德有．1999．中国东部中生代岩浆作用与岩石圈减薄．长春科技大学学报，29(4)：313－318
吴福元，李献华，杨进辉，郑永飞．2007a．花岗岩成因研究的若干问题．岩石学报，23(6)：1217－1238
吴福元，李献华，郑永飞，高山．2007b．Lu-Hf 同位素体系及其岩石学应用．岩石学报，23(2)：185－220
吴福元，徐义刚，高山，郑建平．2008．华北岩石圈减薄与克拉通破坏研究的主要学术争论．岩石学报，24(6)：1145－1174
吴福元，刘小驰，纪伟强，王佳敏，杨雷．2017．高分异花岗岩的识别与研究．中国科学(地球科学)，47(7)：745－765
谢桂青，毛景文，胡瑞忠，李瑞玲，曹建劲．2005．中国东南部中-新生代地球动力学背景若干问题的探讨．地质论评，51(6)：613－620
邢光福，卢清地，陈荣，张正义，聂童春，李龙明，黄家龙，林敏．2008．华南晚中生代构造体制转折结束时限研究——兼与华北燕山地区对比．地质学报，82(4)：451－463
杨经绥，许志琴，吴才来，刘福来，史仁灯，Wooden J，Maruyama S．2002．含柯石英锆石的 SHRIMP U-Pb 定年：胶东印支期超高压变质作用的证据．地质学报，76(3)：354－372

于津海，王德滋，耿建华．1998. 一个古元古代A型流纹岩．地球化学，27(6)：549－558
翟明国，樊祺诚．2002. 华北克拉通中生代下地壳置换：非造山过程的壳幔交换．岩石学报，18(1)：1－8
翟明国，朱日祥，刘建明，孟庆任，侯泉林，胡圣标，李忠，张宏福，刘伟．2003. 华北东部中生代构造体制转折的关键时限．中国科学(D辑)，33(10)：913－920
翟明国，范宏瑞，杨进辉，苗来成．2004. 非造山带型金矿——胶东型金矿的陆内成矿作用．地学前缘，11(1)：85－98
张风霄，周瑶琪，王安东，于姗姗．2015. 山东省灵山岛负载构造和球-枕构造研究．沉积与特提斯地质，35(3)：42－50
张海春，吕洪波，李建国，王俊，张素菁，董晓朋，张星，黄振才，舒云超，任星民．2013. 山东青岛早白垩世新地层单位-灵山岛组．地层学杂志，37(2)：216－222
张旗，王焰，王元龙．2001. 燕山期中国东部高原下地壳组成初探：埃达克质岩Sr、Nd同位素制约．岩石学报，17(4)：505－513
张星，吕洪波，张海春，王俊，张素菁，董晓朋，黄振才，舒云超．2012. 山东胶南灵山岛早白垩世磨拉石地质意义初探．青岛：全国古地理学及沉积学学术会议，159－160
张岳桥．2006. 山东胶莱盆地沉积-岩浆-构造演化序列：对中国东部晚中生代岩石圈减薄过程的制约．南京：全国岩石学与地球动力学研讨会会议摘要，44－46
张岳桥，李金良，张田，董树文，袁嘉音．2008. 胶莱盆地及其邻区白垩纪-古新世沉积构造演化历史及其区域动力学意义．地质学报，82(9)：1229－1257
张振凯，周瑶琪，梁文栋，岳会雯，周腾飞，彭甜明．2016. 山东灵山岛早白垩世构造演化及地质意义．海洋地质前沿，32(4)：1－10
张振凯，周瑶琪，彭甜明，于珊珊，岳会雯，周腾飞，刘加召．2017. 山东灵山岛莱阳群粉砂岩地球化学特征及意义．地球科学，42(3)：357－377
赵广涛，曹钦臣，王德滋，李惠民．1997. 崂山花岗岩锆石U-Pb年龄测定及其意义．青岛海洋大学学报，27(3)：382－388
赵越，陈斌，张拴宏，刘建民，胡健民，刘健，裴军令．2010. 华北克拉通北缘及邻区前燕山期主要地质事件．中国地质，37(4)：900－915
钟建华．2012. 灵山岛中生代沉积岩是深水远源浊积岩、还是陆内三角洲沉积？——与吕洪波教授商榷．地质论评，58(6)：1180－1182
钟建华，倪良田，邵珠福，李勇，刘选，毛毳，刘圣鑫，孙宁亮，陈彬，王凯，罗可，王韶洁，刘闯，刘宝，熊志强．2016. 青岛灵山岛下白垩统风暴岩与风暴沉积的发现及意义．古地理学报，18(3)：381－398
周新华．2009. 北中-新生代大陆岩石圈转型的研究现状与方向——兼评"岩石圈减薄"和"克拉通破坏"．高校地质学报，15(1)：1－15
周瑶琪，张振凯，许红，王安东，魏凯，张云翠，王子阳，李斗，陈阳子，刘扬，于珊珊，高晓军．2015a. 灵山岛沉积物软变形构造特征．海洋地质前沿，31(4)：42－54
周瑶琪，张振凯，梁文栋，李素，岳会雯．2015b. 山东东部晚中生代构造-岩浆活动及原型盆地恢复．地学前缘，22(1)：137－156
周瑶琪，周腾飞，张振凯，梁钊，梁文栋，王安东，于姗姗．2017. 山东省灵山岛下白垩统青山群火山地震软沉积物变形构造特征及成因机制．古地理学报，19(4)：567－582
朱日祥，陈凌，吴福元，刘俊来．2011. 华北克拉通破坏的时间、范围与机制．中国科学(地球科学)，41(5)：583－592
朱日祥，徐义刚，朱光，张宏福，夏群科，郑天愉．2012. 华北克拉通破坏．中国科学(地球科学)，42(8)：1135－1159